PERGAMON

Journal of Structural Geology 25 (2003) 959–982

JOURNAL OF STRUCTURAL GEOLOGY

www.elsevier.com/locate/jstrugeo

Testing models for obliquely plunging lineations in transpression: a natural example and theoretical discussion

Dyanna M. Czeck*, Peter J. Hudleston

Department of Geology and Geophysics, University of Minnesota, Minneapolis, MN 55455, USA

Received 1 December 2000; revised 13 June 2002; accepted 20 June 2002

Abstract

Theory predicts that stretching lineations in an ideal vertical transpressional zone should be either vertical or horizontal. Many field descriptions of transpressional zones, however, indicate a range of lineation orientations between these extremes. Several theoretical models have been developed to explain such departures from expected lineation orientation, and we discuss these in the context of a field example from the Archean Superior Province in the North American craton. Existing models are insufficient to explain obliquely plunging lineations in this example because: (1) obliquely plunging lineations cannot be accounted for by shear zone boundary effects imposed by a no-slip condition, (2) foliations and lineations vary independently, (3) the vorticity-normal section is subhorizontal, limiting possibilities for inclined simple shear, (4) high vorticity is needed for finite strains and lineations to match previously proposed triclinic models, but vorticity is relatively low, and (5) juxtaposed east and west plunging lineations are unlikely in the previously proposed triclinic models. Because existing theoretical models are not applicable to our field example, we contemplate a new model to explain obliquely plunging lineations within quasi homogeneous transpression.

Keywords: Transpression; Kinematic model; Lineation; Foliation; Seine conglomerates

1. Introduction

The term ‘transpression’ was first introduced by Harland (1971) to describe obliquely convergent motion between two crustal blocks, or motion partitioned into convergence and strike-slip. Sanderson and Marchini (1984) provided a mathematical description of a specialized case of transpression: homogeneous deformation consisting of orthogonal simple shear and pure shear components. As discussed by Robin and Cruden (1994), a dual meaning for ‘transpression’ has developed in the literature following the Sanderson and Marchini contribution. Harland’s original definition required only a tectonic constraint of oblique convergence. This oblique convergence may be accommodated in many ways, including the partitioning between folds and faults that Harland presented. In contrast, Sanderson and Marchini gave a definition of transpression with specific kinematic constraints that is a subset of transpression as described by Harland. In addition to orthogonal simple shear and pure shear components, their model involves constant volume and confines deformation to a vertically bounded zone. Such an idealized scenario is, perhaps, most likely to correspond to strain in deep, vertical ductile shear zones.

Fossen and Tikoff (1993) divided transpression in the Sanderson and Marchini sense into pure-shear-dominated and simple-shear-dominated, depending on the angle of convergence and defined by the infinitesimal strain. The structural fabrics predicted in such transpression are illustrated in Fig. 1. Pure-shear-dominated and simple-shear-dominated transpression may be differentiated using W_k (Fossen and Tikoff, 1993), Truesdell’s kinematic vorticity number (Truesdell, 1954, p. 107). In pure shear dominated transpression ($0 < W_k \leq 0.81$), the stretching lineation is always vertical; in wrench dominated transpression ($0.81 < W_k < 1$), the stretching lineation starts horizontal and switches to vertical after some finite amount of strain (Fossen and Tikoff, 1993). The strain at which this switch occurs increases with

* Corresponding author. Present address: Department of Geoscience, Indiana University of Pennsylvania, 115 Walsh Hall, Indiana, PA 15705, USA.

E-mail address: dyanna@iup.edu (D.M. Czeck).

0191-8141/03/$ - see front matter © 2002 Elsevier Science Ltd. All rights reserved.
PII: S0191-8141(02)00079-2

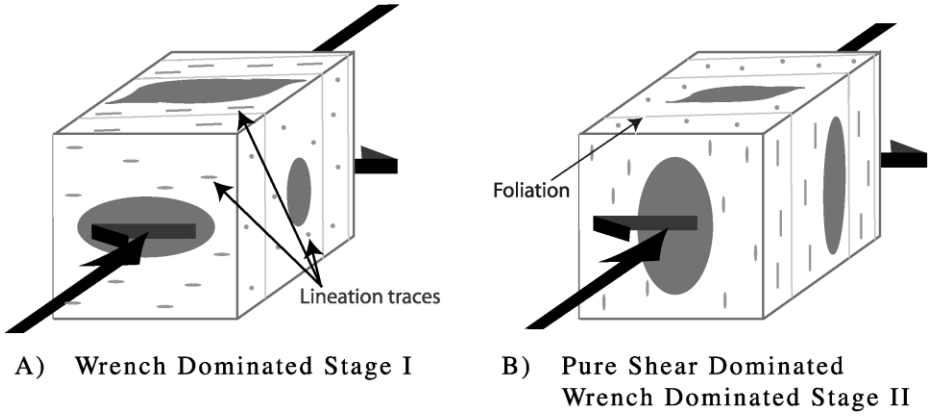

Fig. 1. Generalized transpression. Strain (simple shear and pure shear components) and fabrics (foliation, lineation, conglomerate clast asymmetry) based on Sanderson and Marchini (1984) and Fossen and Tikoff (1993). The front and back sides of the boxes are parallel to the deformation zone boundaries. The mineral fabrics are shown in the general case with fabric oblique to the deformation zone boundaries. As strain accumulates, the foliation becomes progressively closer to subparallel with the deformation zone boundaries. Ellipses (some with 'tails') represent schematic clast traces on each plane.

increasing W_k, but the switch occurs instantaneously. The lineation switch is due to the way in which strain accumulates. Pure shear accumulates strain more efficiently than simple shear; so late stage deformation fabrics will be dominated by the pure shear component of strain. In either case, regardless of the convergence angle or amount of strain, basic transpression (in the Sanderson and Marchini sense) requires that the stretching lineation (X) be only vertical or horizontal.

Despite the theoretical predictions, many field examples of what otherwise appear to be transpressional environments show a range of obliquity of the lineation (Schultz-Ela and Hudleston, 1991; Robin and Cruden, 1994; Goodwin and Williams, 1996; Dutton, 1997; Jones et al., 1997; Lin et al., 1998). For our study, we explore how such obliquely plunging lineations could form within a bulk transpressional regime. The question has been addressed in various ways by different authors (Robin and Cruden, 1994; Merle and Gapais, 1997; Jiang and Williams, 1998; Lin et al., 1998). We will examine their models in this paper and emphasize ways to test applicability of such models to a field setting.

In the present study, a field example from the western Superior Province of the North American craton is presented and its tectonic fabrics are compared with those predicted for theoretical models of obliquely plunging lineations in transpression. Our field area is well-suited for the type of study because it possesses a range of obliquely plunging lineations in conjunction with the primary structural features of areas interpreted to have undergone transpression: steep foliation, flattening strain, and asymmetric shear indicators on the subhorizontal planes of outcrops. Our study is unique because it evaluates the validity of obliquely plunging lineation models for a particular field site by integrating multiple lines of fabric evidence: orientation of foliation and lineation, spatial distribution of foliation and lineation, orientation of the vorticity-normal section, and finite strain magnitude.

2. Obliquely plunging lineations along the Wabigoon–Quetico boundary

2.1. Geologic setting

The Superior Province (Fig. 2) is the world's largest contiguous Archean terrane. It consists of subprovinces defined by lithological differences, metamorphic grade, and structural boundaries (Card and Ciesielski, 1986). The central portion of the Superior Province is defined by alternating volcano-plutonic and metasedimentary subprovinces. A popular tectonic model for these subprovinces consists of arc sequences (metavolcanics) and their corresponding accretionary prism sequences (metasediments) that were amalgamated during repeated island arc collisions at about 2.7 Ga (Burke et al., 1976; Langford and Morin, 1976; Hoffman, 1989; Card, 1990; Hoffman, 1990). The obliquity of these collisions and the transpressional nature of the boundary are evident by the general structural fabric of the region with vertical foliations and flattening fabrics in tandem with asymmetric shear sense indicators on the subhorizontal plane (Poulsen, 1986; Tabor and Hudleston, 1991; Borradaile and Dehls, 1993; Borradaile et al., 1993; Czeck, 2001).

In particular, we focus here on the boundary region between the Quetico metasedimentary subprovince and the Wabigoon metavolcanic subprovince in the western Superior Province. The Quetico contains mostly amphibolite facies metasedimentary rocks, and the Wabigoon contains mostly greenschist facies metavolcanic rocks. While the whole boundary may possibly be considered to have undergone transpression, we concentrate on the vicinity near Mine Centre, Ontario because of the presence

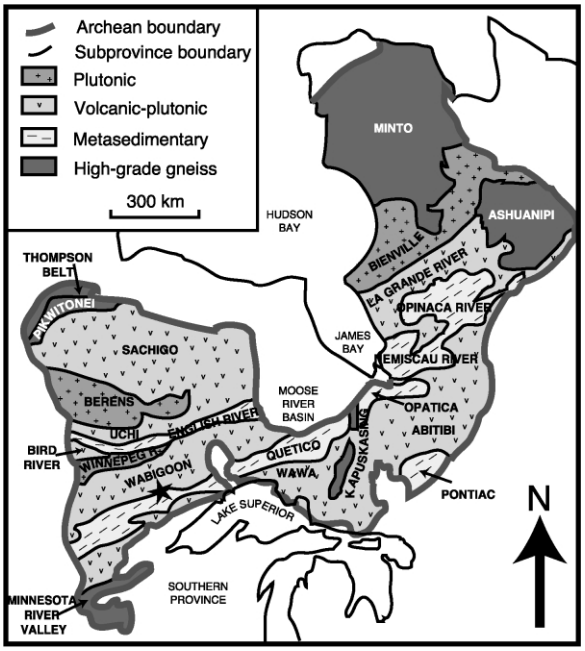

Fig. 2. Generalized view of the Superior Province, North America (Card and Ciesielski, 1986). The area along the Wabigoon–Quetico boundary described in this study is indicated by a star.

of the distinctive Seine River Metasedimentary Group that includes the polymictic Seine River conglomerates (Fig. 3). The conglomerates are relatively immature, clast supported, and polymictic with mostly volcanic or plutonic clast lithologies (Wood, 1980; Frantes, 1987). The matrix has an intermediate volcanic composition (Frantes, 1987, p. 58). From stratigraphic evidence, the Seine River conglomerates are thought to have formed after the deposition of the volcanic sequences (Poulsen et al., 1980). Absolute dating of zircons have confirmed this (Davis et al., 1989; Fralick and Davis, 1999). The Seine Group conglomerates may have formed synkinematically during relatively early stages of collision, possibly in structures similar to pull-apart basins (Poulsen, 1986).

2.2. Structural geometry

The Wabigoon–Quetico boundary may have a similar deformation history to other subprovince boundaries within the Superior Province. The adjacent subprovince boundary to the south, between the metavolcanic Wawa subprovince and metasedimentary Quetico subprovince, contains fabric evidence for an early deformation of recumbent nappe folding and a more ubiquitous overprinting of a ductile subvertical flattening fabric and near vertical shear zones that have been attributed to dextral transpression (Hooper and Ojakangas, 1971; Bauer, 1985; Hudleston et al., 1988). Previous structural work along the Wabigoon–Quetico boundary indicates a similar strain history, as evidenced by a subvertical foliation overprinting large folds (Poulsen, 1986; Tabor and Hudleston, 1991). Despite evidence for initial folding along the Wabigoon–Quetico boundary (Poulsen, 1986; Tabor and Hudleston, 1991), the dominant fabrics observed in the field seem to relate to the ductile transpressional event. Many authors have described the Wabigoon–Quetico boundary as kinematically transpressional in nature, based on the strong flattening fabrics and asymmetric features consistent with simple shear in the subhorizontal plane (Poulsen, 1986; Tabor and Hudleston, 1991; Borradaile and Dehls, 1993; Borradaile et al., 1993).

The conglomerate, having been deposited late in the deformation history, did not undergo the major early folding that occurred elsewhere along the boundary (Poulsen, 1986; Davis et al., 1989). Field observations indicate that folds are sparse within the Seine Group conglomerates, and where minor folds can be observed, it is apparent that the foliation is not associated with folding. In detail, there is only evidence for one set of structural fabrics, with no evidence for multiple overprinting foliations. For these reasons, we interpret the dominant fabrics within the Seine conglomerates to be the result of only one major regional ductile deformation.

Strain is pervasive throughout the entire Wabigoon–Quetico boundary zone, but it is also localized into an anastomosing network of more discrete shear zones, including two main zones of localized shear and displacement. These are the Seine River–Rainy Lake Shear Zone and the Quetico Shear Zone, which diverge to the west and merge to the east (Fig. 3). An anastomosing pattern of smaller shear zones link the major shear zones shown in Fig. 3 (Poulsen, 1986). This pattern represents a broad zone of wrenching and not merely a local zone of late faulting (Poulsen, 1986). The presence of discrete shear zones implies some strain partitioning between the pure shear and simple shear components along the Wabigoon–Quetico boundary. We surmise that the discrete shear zones are zones with relatively high simple shear influence. Conversely, we suppose that the wide zones of deformation between the shear zones have undergone deformation with stronger pure shear influence.

2.3. Structural fabrics

Strongly foliated rocks within all of the lithologies (excepting some late stage plutons) characterize the Wabigoon–Quetico boundary. The foliations are largely subvertical and at a low angle to the subprovince boundary (Fig. 4b). Typically, chlorite or amphibole forms the mineral lineation, which varies in intensity from weak to strong depending on location. Its plunge is quite variable across the Wabigoon–Quetico boundary without any systematic change from east to west or from north to south (Figs. 3 and 4a), although there are local domains of similar lineation plunge. There is a concentration of mineral lineations plunging steeply to the east; however, there are also significant components of westward and shallowly plunging lineations as well. The overall dominance of the

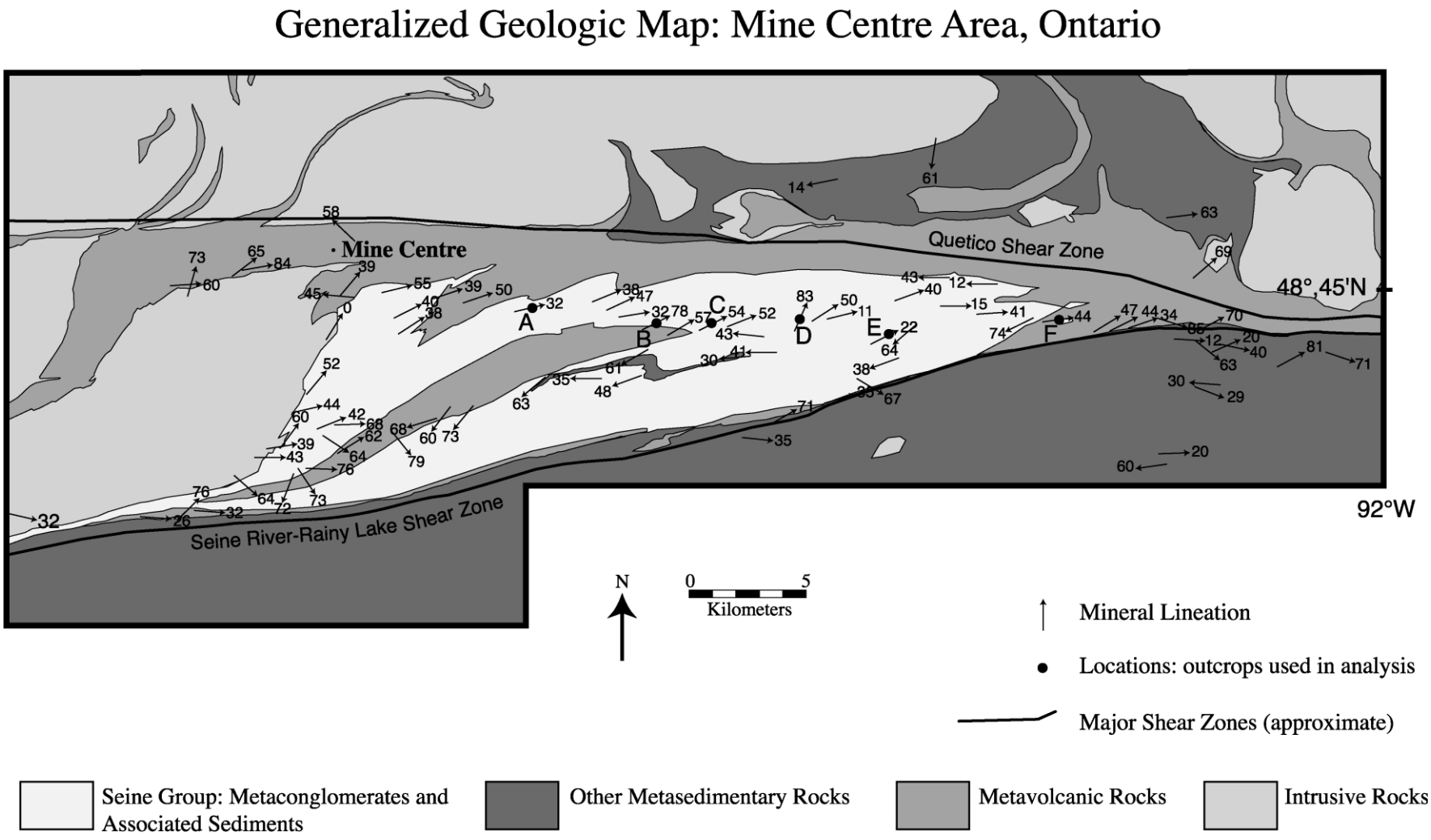

Fig. 3. Generalized geologic map of Wabigoon–Quetico Subprovince boundary including representative stretching lineations (based on Wood et al., 1980a,b; Stone et al., 1997a,b; and this study.)

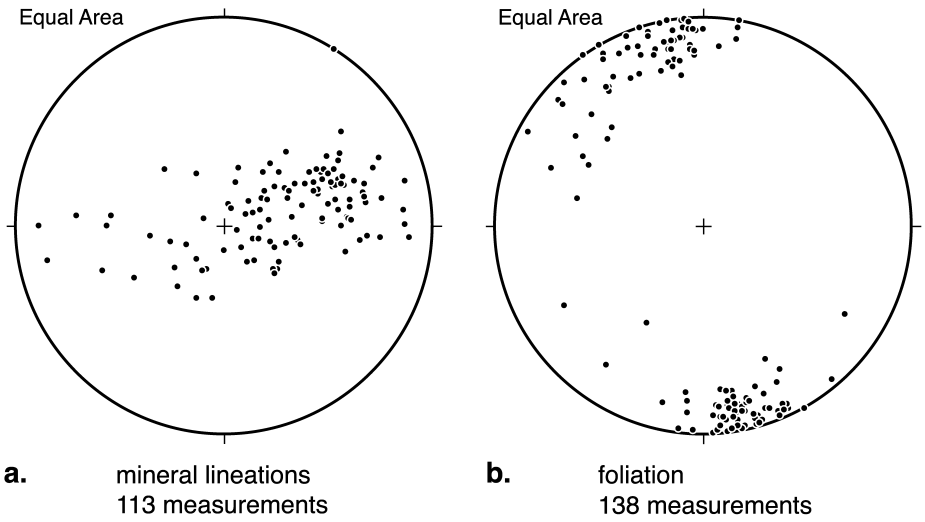

Fig. 4. Equal area stereonets representing structural fabric of the Wabigoon–Quetico Subprovince boundary. (a) Stretching (mineral) lineations. (b) Poles to foliation.

foliation over the lineation creates an S–L type fabric (Flinn, 1965).

Most rock fabric features along the boundary are consistent with transpression. The foliation is subvertical (Fig. 4b), and the individual clasts within the Seine River conglomerates display a subvertical flattening fabric evidenced by their oblate shape. On subhorizontal planes, the clasts commonly form dextral shear sense indicators (Fig. 5), regardless of lineation orientation. This asymmetry is not observed in other orientations. The consistency of these fabrics with the homogeneous transpression model suggests that at least the majority of the Wabigoon–Quetico boundary has undergone quasi homogeneous transpression.

Significantly, however, the mineral lineations are neither vertical nor horizontal as predicted by the general transpression model (Fig. 1); they plunge between 0 and 90° in both east and west directions (Fig. 4a). There is a concentration of mineral lineations that plunge approximately 45° to the east; however, there are a significant number of lineations that deviate far from this orientation. The lineations do seem to cluster into domains; however, the pattern of lineation orientations cannot be explained by a folding event (Czeck, 2001). Although the mineral lineation is locally perturbed by rigid conglomerate clasts, the range of obliquely plunging orientations is not due only to this phenomenon. A consistent, average, penetrative lineation can be seen at the outcrop scale. Typically, the lineations are consistent within approximately a 1 km scale. Therefore, the variation in lineations is not caused by small-scale phenomena, but must have a larger-scale cause. The range of lineation plunges within the conglomerate makes this an ideal place to test the various models that predict obliquely plunging lineations in transpression.

Although we have referred thus far to a single lineation in these rocks, in fact, two distinct linear elements can be measured independently within the Seine conglomerate: the mineral lineation and the lineation defined by the long axes of the conglomerate clasts. Both can be considered penetrative features of the rock fabric. From qualitative observations, we can state that the long axes of the clasts within the Seine River conglomerate are generally coincident with the mineral lineation (Fig. 5a). This correlation between the finite strain axis X and mineral lineation strongly supports the assumption that the foliation and lineation mineral fabrics accurately record finite strain (e.g. Ramsay, 1967, p. 181; Goodwin and Williams, 1996; Tikoff and Greene, 1997). Such a correlation is more robustly tested with strain analysis reported in this study.

The presence of the Seine River conglomerate provides a distinct advantage to studying obliquely plunging lineations along a transpressional boundary. Most transpression studies along major terrane boundaries are able to distinguish the orientation of the finite strain ellipsoid only indirectly through foliation and lineation measurements. There is evidence to support such an approach. Strain data is relatively sparse, so where there can be shown to be a relationship between strain and foliation and lineation measurements, foliation and lineation may be used as a proxy for XY, and X orientations of the strain ellipsoid, respectively. Many studies have shown that the XY plane of cumulative strain is parallel to the cleavage in deformed rocks in many circumstances (e.g. Flinn, 1965; Ramsay, 1967, p. 181). Similarly, numerous studies have shown that the X direction of cumulative strain is parallel to the mineral lineation (e.g. Ramsay, 1967, p. 181; Goodwin and Williams, 1996; Tikoff and Greene, 1997). It is difficult to relate mineral fabric to strain magnitude and symmetry, although in a qualitative sense this has been done (Flinn, 1965).

The relationship between mineral fabrics and finite strain for the conglomerates is examined in this study. Although the correlation between mineral fabrics and finite strain is

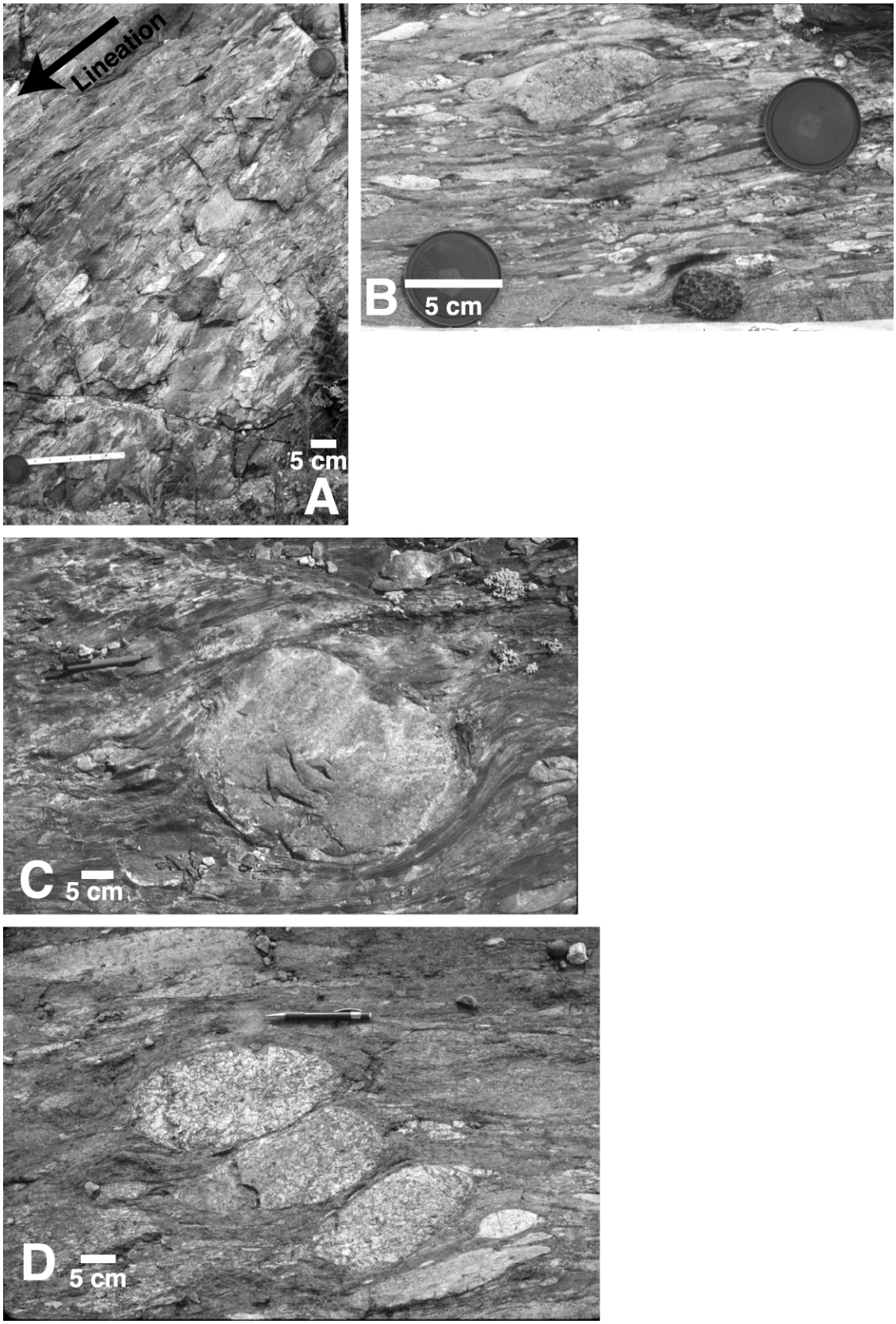

Fig. 5. Photographs of the Seine River Metaconglomerate. (A) Foliation plane. Long axes of clasts generally coincide with stretching (mineral) lineation observed in rock. (B–D) Subhorizontal surfaces. Asymmetric features including pressure shadows formed at tips of more rigid clasts, rotated rigid clasts, and clast tiling indicate dextral sense of shear.

generally good, this may not always be the case. The direct relationship between observed mineral fabrics and finite strain is an assumption that should be tested when possible. By using the conglomerates as finite strain recorders, measured strain can be compared with mineral fabrics to determine the extent to which the finite strain ellipsoid orientation matches the mineral fabric. Furthermore, the conglomerates, as strain recorders, allow us to determine the finite strain ellipsoid shape, a measure that represents strain magnitude and eccentricity in addition to the direction of finite strain. The finite strain magnitudes provide additional constraints with which to test transpression models.

2.4. Quantification of strain

In strain analysis, a deformed object or population of objects of known initial shape or shape distribution, like a conglomerate clast or clasts, is measured and in effect mathematically 'undeformed' to quantify strain. Comprehensive strain analysis of the Seine River Conglomerates was conducted at six representative outcrops in order to allow finite strain magnitudes and orientations to be used to further constrain obliquely plunging lineation models. These specific outcrops were chosen because, based on observation, they displayed a range of strain magnitudes. In all cases, the foliation was steep and the lineation plunged eastwards to varying amounts. Strain analysis in our study was conducted using the following procedure.

The locations for strain analyses were chosen from road exposures along Ontario Highway 11, because these exposures allow a three-dimensional view of the clasts that are generally too large to analyze in hand specimen. For each outcrop, several oriented photographs were taken of the foliation plane, planes approximately perpendicular to foliation and parallel to lineation, and planes roughly perpendicular to each of these. Thus, we generated 6–11 oriented rock surface photographs of each outcrop. It is important to note that these photographs, although selected to be as close to mutually perpendicular as possible, are not oriented parallel to the principal planes of strain.

As the Seine River conglomerate is polymictic, one might expect significant differences in clast strain magnitude based on the rheological contrasts between the clasts and matrix. Therefore, clasts were divided into separate lithological groups based on potential rheological similarity: granitoids, quartzites, felsic volcanics, and intermediate-mafic volcanics.

There is often a ductility contrast between the clasts and matrix in a conglomerate. In the case of polymictic conglomerates such as the Seine River conglomerates, ductility contrasts are highly variable and complex. In general, clasts that are stiffer than the matrix will record less strain and clasts that are less stiff than the matrix will record more strain than the rock as a whole. Even if reliable strain of each clast type and matrix could be determined, the whole rock strain is not obvious, because it depends on the compositional proportion of various clasts and matrix and the effect this has on the recorded strain.

Competency contrasts, such as those between matrix and pebbles in a conglomerate, have an important impact on the resultant deformation. A sizeable volume of literature addresses the theoretical deformation of a spherical or ellipsoidal inclusion within a contrasting matrix (Eshelby, 1957; Gay, 1968a,b; Bilby et al., 1975; Bilby and Kolbuszewski, 1977; Lisle et al., 1983; Lisle, 1985; Freeman, 1987). Other authors have extended such theoretical deformation to nonellipsoidal inclusions (Treagus et al., 1996; Treagus and Lan, 2000). In most of these studies, the authors have considered deformation in Newtonian materials and have shown that an inclusion with a contrasting viscosity to the matrix will deform with a different strain than the bulk strain. This theory has been applied, in particular, to deformed conglomerates in order to use various viscosity ratios (Newtonian) to determine finite strain (Gay, 1968b, 1969; Huber-Aleffi, 1982; Lisle et al., 1983; Freeman and Lisle, 1987). This approach works best when the viscosity ratio between the pebble and matrix is small (Freeman and Lisle, 1987). Microstructural evidence for non-Newtonian deformation in conglomerates and the impact on the final strain has been considered by some authors (Etheridge and Vernon, 1981; White, 1982), but considerable future work is needed in this area.

Due to the complexities of having clasts of different viscosity and the bulk compositional heterogeneity of the conglomerate across its basin, we will take a simplified approach to quantifying conglomerate strain in this paper. The strain analysis for the intermediate-mafic volcanic clasts is used here to approximate whole rock strain for the Seine River conglomerates. This approach seems reasonable in this case because of the compositional similarity between the matrix and these clasts and the large percentage of volcanic clasts in the rock.

Despite the need to make assumptions about the initial shape and fabric of the conglomerate clasts, they have proved to be useful recorders of finite strain (Holst, 1982; Ramsay and Huber, 1983, p. 197). We assume here that the clasts were originally ellipsoidal in shape and randomly oriented. Even though bedding is evident in some locations, the assumption of random fabric was made to decrease the judgment of the investigator that is needed of strain analysis if bedding information is included (Lisle, 1985). Holst (1982) gave justification for such an approach. Also, the assumption of random fabric is justified because the computed finite strain ellipsoid orientation matches the ellipsoid orientation presumed from the foliation and mineral lineation orientation (Fig. 6). If there were a strong initial fabric in the conglomerate clasts, in general, the finite strain recorded by these clasts would not match the mineral fabric.

Strain measurements were carried out using standard techniques on meter-scale, two-dimensional surfaces. At each outcrop, numerous planes, subject to availability, were

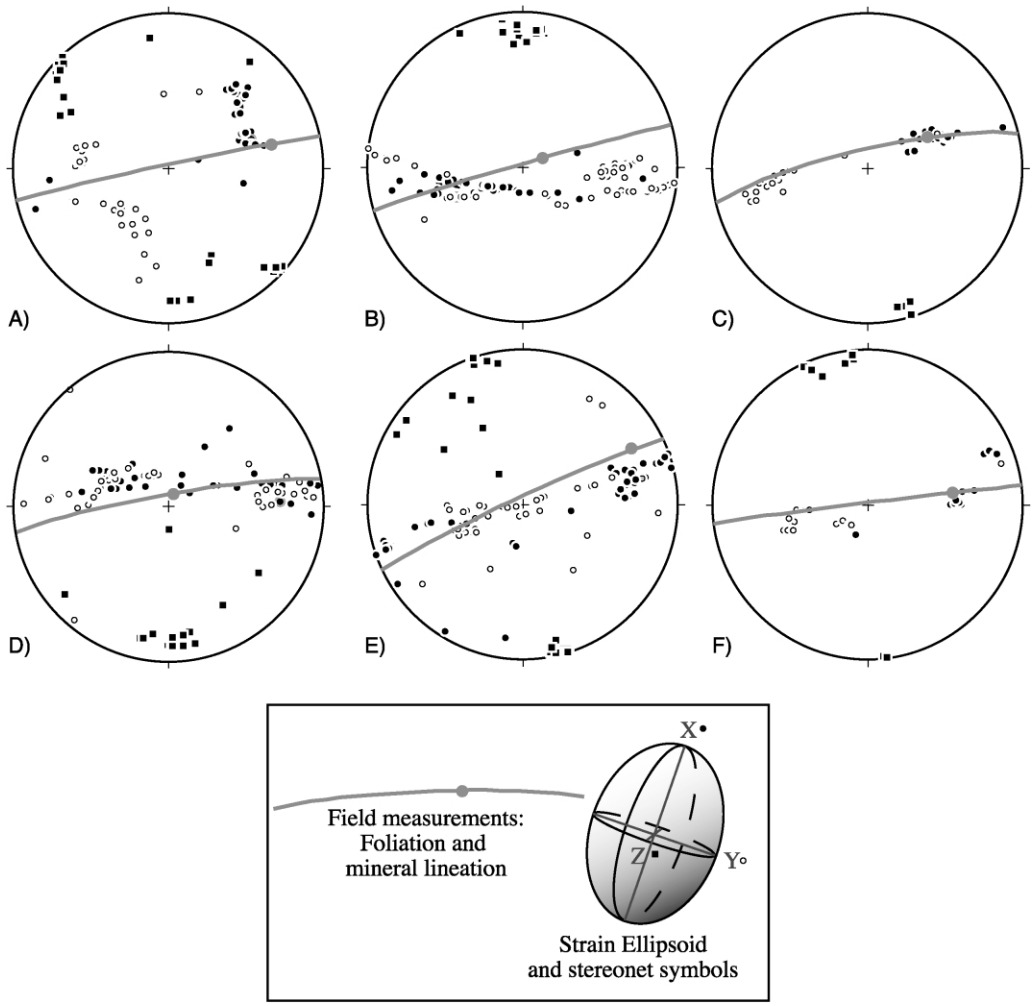

Fig. 6. Equal area stereonets indicating strain analysis solutions and fabric measured in the field for six representative outcrops. *X*, *Y*, and *Z* correspond to principal axes of the strain ellipsoid. Fabrics measured in the field include foliation and mineral (stretching) lineation. (A)–(F) represent data from outcrops A–F, respectively.

photographed and analyzed. The axes (lengths and orientations) of the clasts were measured. The harmonic mean of axial ratios was used to represent the average strain on each two-dimensional photograph (Lisle, 1979).

In order to calculate the three-dimensional strain, combinations of three planes were used. The planes available at the outcrops were not principal planes or even exactly mutually orthogonal. To calculate three-dimensional strains, we combined two-dimensional strain results from groups of three approximately orthogonal planes. These two-dimensional results were input into a strain program that utilizes the least squares method for randomly oriented planes (Shimamoto and Ikeda, 1976; Owens, 1984), but does not include the iterative process described by Owens (1984) to reduce the solutions to an ultimate best-fit ellipsoid. The planes were selected based on their proximity to mutual orthogonality in order to generate calculated ellipsoids with the best possible mathematical fits. For each set of three planes, six possible ellipsoid solutions are generated (for explanation, see Shimamoto and Ikeda (1976) and Owens (1984)). The robustness of a solution depends on several factors including the number of measurements (which is highly variable due to the inconsistent number of clasts on each two-dimensional plane) and the relative degree of confidence in the three-dimensional mathematical fits. In order not to weigh these unrelated factors inappropriately, all solutions were kept at this point in the process in order to eliminate bias by the investigator. The process results in 54–72 ellipsoid 'solutions' for each outcrop. For each outcrop, the solutions are displayed on a natural log Flinn diagram that is divided into equal regions. The number of solutions falling within that region is indicated (Fig. 7).

To determine the 'best-fit' strain ellipsoid for an outcrop, we assumed that the most robust solutions, those based on the most measurements and those with the best mathematical ellipsoid fits, would cluster together. The least reliable solutions should be scattered. Therefore, the Flinn plot region with the highest density of solutions is used here to approximate the strain (Fig. 7).

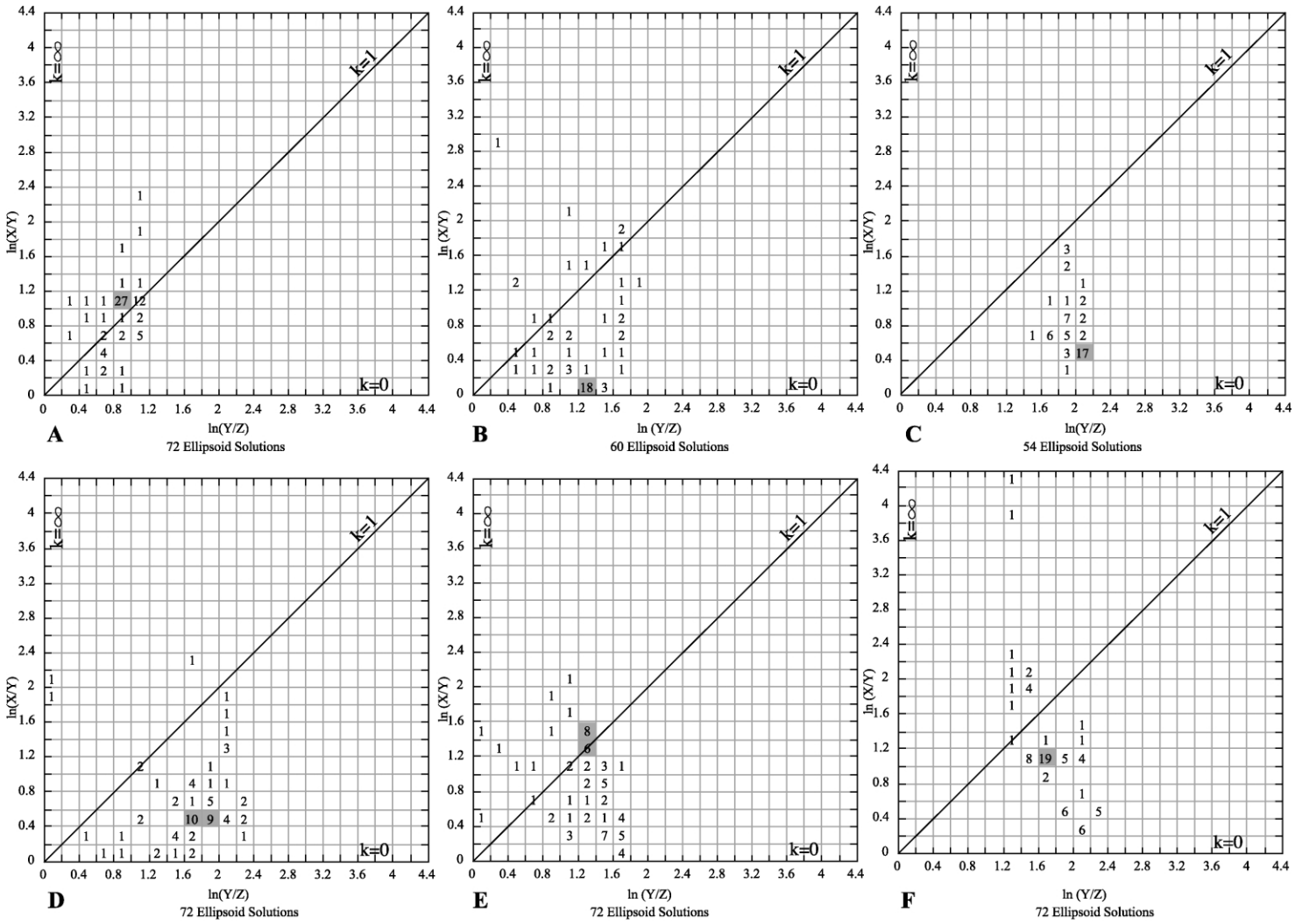

Fig. 7. Natural log Flinn diagrams showing all calculated three-dimensional strain solutions for each representative outcrop. The data is represented by a number corresponding to the number of solutions falling within the Flinn diagram grid. The average solution was taken to be the center of the grid element with the most calculated solutions. (A)–(F) represent data from outcrops A–F, respectively.

Table 1
Summary of strain analysis results for six representative outcrops. *X*, *Y*, and *Z* are the principal axes of the strain ellipsoid. Strain ellipsoid shapes are described by lengths of the principal axes or ν = Lode's parameter and the parameter $\bar{\epsilon}_s$ (e.g. Hossack, 1968)

	Foliation	Mineral lineation	Calculated principal axes	Trend	Plunge	Principal axes lengths	ν	$\bar{\epsilon}_s$
A (west)	078, 88N	077, 32					−0.09	1.43
			X	66	45	7.5		
			Y	267	44	2.5		
			Z	167	11	1		
B	074, 88N	065, 78					0.81	1.08
			X	244	60	4		
			Y	104	26	3.5		
			Z	358	12	1		
C	077, 80N	063, 54					0.60	1.95
			X	65	52	13.5		
			Y	262	38	8		
			Z	166	8	1		
D	080, 84N	024, 83					0.55	1.63
			X	67	53	9		
			Y	278	33	5.5		
			Z	178	15	1		
E	065, 86N	063, 22					−0.10	1.96
			X	75	23	16		
			Y	246	67	3.5		
			Z	343	3	1		
F (east)	083, 89N	082, 44					0.26	1.94
			X	81	36	15		
			Y	257	54	5.5		
			Z	350	2	1		

The results of the strain analysis are shown in Table 1 for the representative outcrops. The parameter $\bar{\epsilon}_s$ (e.g. Hossack, 1968) was used as a measurement of strain magnitude. In general, the differences in strain magnitude are not great. In part, this may be due to the inherent underestimation of strain in highly deformed rocks. In the highest strained rocks, the distinction between clast and matrix becomes obscured. Thus, the strain measurements are somewhat biased to the lesser deformed clasts.

Strain analysis indicates that rocks at each of the outcrops have different positions in the Flinn diagram and thus have likely undergone slightly different strain histories (Fig. 7). The rocks at two outcrops, A and E, have undergone deformation most closely resembling plane strain, with Flinn's $k \approx 1$ (see Ramsay (1967, p. 137) for definition of k). The rocks at four outcrops, B, C, D, and F, have undergone various amounts of flattening strain with Flinn's $k < 1$. The latter four outcrops have an oblate strain shape, consistent with what one would expect in homogeneous ductile transpression. The results from the former two outcrops are only likely to occur in transpression if one of the deformation components (pure shear or simple shear) dominates so that the resulting strain closely resembles plane strain.

Outcrops C, E, and F have undergone the highest strain with $\bar{\epsilon}_s \approx 1.95$. These rocks have very different positions on the Flinn plot, indicating plane strain or flattening. This phenomenon may be a reflection of different strain paths within the boundary zone. The differences in strains and possibly strain paths between the various locations may well be significant, but for the purposes of testing models, we will consider the strain magnitudes and fabrics only within individual outcrops. It is possible, for example, that a theoretical model could be consistent with these different strain histories if the model is applied individually to each location, such that the relative amounts of pure shear and simple shear may vary across the deformed area. Whether the individual strain histories are mutually compatible is another matter.

3. Models for obliquely plunging lineations in transpression

In order to account for obliquely plunging lineations in transpression, previous authors have described models in which the orientation of the simple shear component deviates in prescribed ways from the generic transpression model of Fig. 1.

As is appropriate for the Wabigoon–Quetico boundary, we discuss here models that predict obliquely plunging lineations in a framework of bulk homogenous kinematic transpression in a steeply dipping to vertical panel similar to that described by Sanderson and Marchini (1984). Other models, otherwise attractive, deviate from this condition in ways that make them inappropriate. For example, the model by Merle and Gapais (1997) predicts fabrics with the geometry of complex flower structures when two simple

shears, thrust and wrench, are combined. In this model, the obliquely plunging lineations occur within a generally dipping deformation zone. This model is not appropriate for our field example because the foliation is subvertical.

3.1. Overall homogeneous transpression with no-slip boundary condition

Robin and Cruden (1994) modified the basic transpression model of Sanderson and Marchini (1984) to include a no-slip condition in the vertical direction as well as the horizontal direction (Fig. 8c and d). The additional no-slip condition creates a bulge on the top, free boundary of the transpression zone, rather than a discrete deforming block moving upwards between rigid walls as shown in Fig. 8a. The analysis by Robin and Cruden was done in terms of instantaneous strain, which does not describe finite strain fabrics. However, their model has been extended to finite strain and fabrics by Dutton (1997). Dutton showed that the boundary conditions along the edge of the transpressional zone create oblique and variable foliations and lineations. Thus, the lineation orientations vary both horizontally and vertically in a systematic way across the deformation zone. The departure of the foliation and lineation fabrics from predicted vertical or horizontal orientations due to the no-slip boundary condition are linked in the Robin and Cruden/Dutton model such that one should not observe an obliquely plunging lineation without an obliquely dipping foliation.

As the foliations within the conglomerates along the Wabigoon–Quetico boundary are consistently subvertical, despite wide variations in lineation plunge, the no-slip boundary condition of the Robin and Cruden model, in which foliations and lineations vary together systematically, cannot provide an adequate explanation of the fabric. The obliquely plunging lineations within the Wabigoon–Quetico subprovince boundary are distributed across the region and do not seem to be restricted to the boundary areas. Moreover, the highest strained areas along the Wabigoon–Quetico boundary do not have vertical or horizontal lineations as predicted in the Sanderson and Marchini and no-slip Robin and Cruden/Dutton models. Therefore, we will turn our attention to models that incorporate oblique simple shear with respect to the strike of the shear zone boundary. Such models include the Robin and Cruden (1994) model when their parameter $\beta \neq 0$ or 90° and the triclinic model proposed by Jones and Holdsworth (1998) and Lin et al. (1998).

3.2. Oblique simple shear in transpression

In the Robin and Cruden (1994) contribution, they recognized a variation in transpression where the simple shear direction is oblique to the strike of the shear zone boundary (when their parameter $\beta \neq 0$ or 90°). Dutton (1997) determined finite fabrics for such deformations. Transpression with an oblique simple shear direction is also discussed by Jones and Holdsworth (1998) and Lin et al. (1998) without the no-slip boundary condition.

Lin et al. (1998) numerically simulated obliquely plunging lineations within a transpressional zone by modeling a type of triclinic transpression, which is essentially the same as the model described by Jones and Holdsworth (1998). Their model includes an oblique angle (ϕ) between the strike of the shear zone boundary and the direction of the bulk simple shear component (Fig. 8e). In this model, the angle ϕ is due to the boundary conditions and is constant across the deformation zone. The relative obliquity of the simple shear creates obliquely plunging lineations (Figs. 8f, 9 and 10). Jiang and Williams (1998) modeled the same triclinic transpression including the effects of volume change. These models can be used in the general case of dipping shear zone boundaries, but they have been specifically described for vertical deformation zones. The general steady-state deformation matrix for the triclinic transpressions described is (Lin et al., 1998, their Eq. 6a):

$$D = \begin{pmatrix} 1 & \frac{\dot{\gamma}}{\dot{\epsilon}}\cos\phi[1-\exp(-\dot{\epsilon}t)] & 0 \\ 0 & \exp(-\dot{\epsilon}t) & 0 \\ 0 & \frac{\dot{\gamma}}{\dot{\epsilon}}\sin\phi\sinh(\dot{\epsilon}t) & \exp(\dot{\epsilon}t) \end{pmatrix}, \quad (1)$$

where $\dot{\gamma}$ = simple shear rate parallel to zone boundary, $\dot{\epsilon}$ = pure shear rate normal to zone boundary, ϕ = angle between the direction of the simple shear strain component and the strike of the zone boundary, and t = time.

3.2.1. Controls on lineation orientation

Deformation paths for the class of triclinic transpression described by Jones and Holdsworth (1998) and Lin et al. (1998) are traced for ratios of simple shear rate to pure shear rate given by $\dot{\gamma}/\dot{\epsilon} = 1, 2, 4, 6, 20$ (Lin et al., 1998). The kinematic vorticity number, W_k, may be used to characterize the noncoaxiality of the deformation. It is given by (Lin et al., 1998, their Eq. 4):

$$W_k = \frac{\dot{\gamma}}{\dot{\epsilon}}\left[4 + \left(\frac{\dot{\gamma}}{\dot{\epsilon}}\right)^2\right]^{-\frac{1}{2}}. \quad (2)$$

This is calculated for each case modeled, and for $\dot{\gamma}/\dot{\epsilon} = 1$, 2, 4, 6, and 20, $W_k = 0.447$, 0.707, 0.894, 0.949, and 0.995, respectively. Notice that if these deformations occurred within a monoclinic transpressional geometry, $\dot{\gamma}/\dot{\epsilon} = 4$, 6, and 20 would describe strongly wrench-dominated transpressions, based on the value of W_k. Note also, however, that the 'pure shear dominated' or 'simple shear dominated' terminology introduced by Fossen and Tikoff (1993) does not apply here unless $\phi = 0$ because the pure shear and simple shear components are not orthogonal, and thus there is no sudden switch between vertical and horizontal lineations. Instead, there is a gradual change from an obliquely

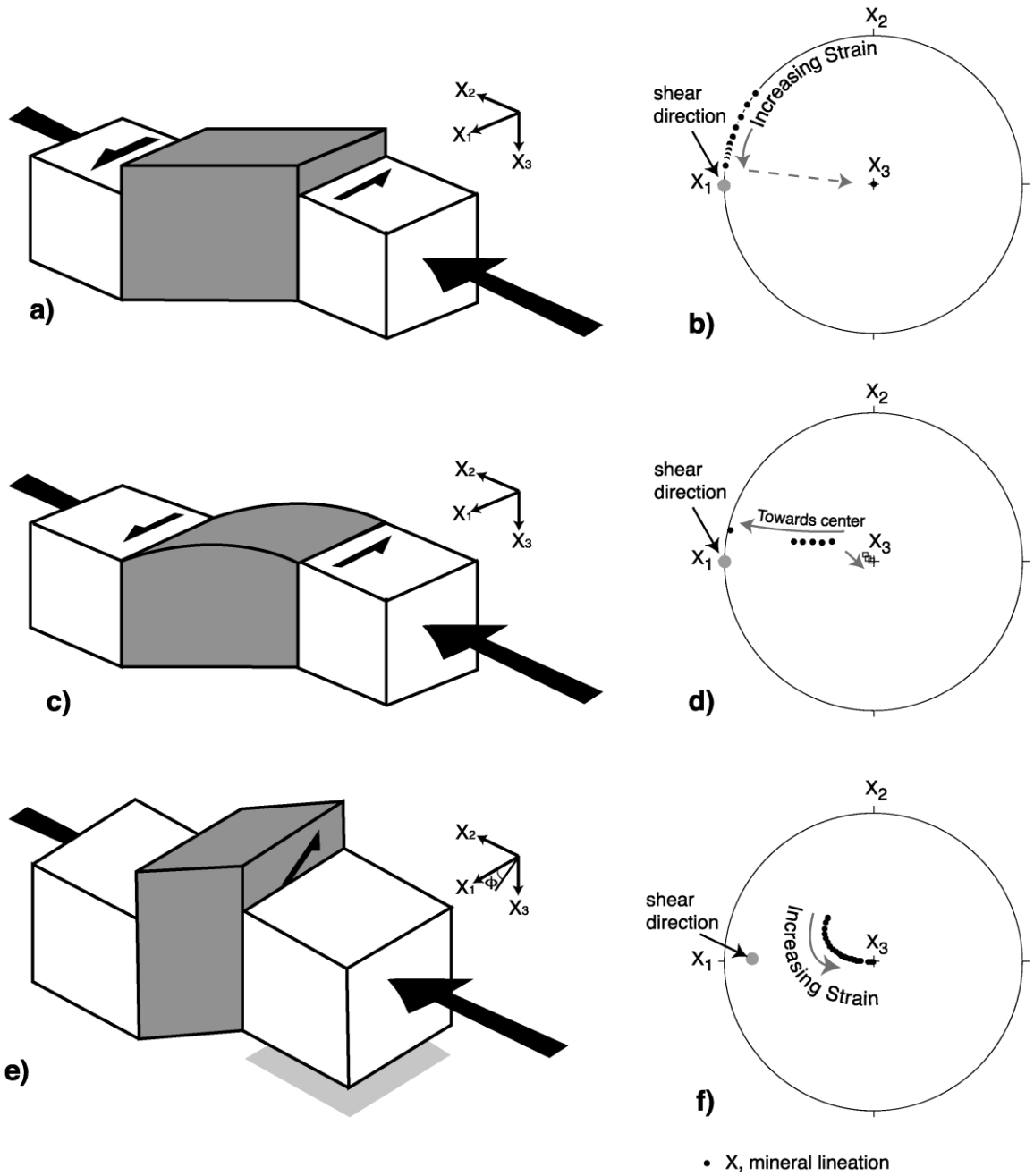

Fig. 8. Transpression Models. (a) Idealized monoclinic transpression model based on Sanderson and Marchini (1984). (b) Stereonet shows one example of lineation orientation with increasing strain (wrench dominated with $W_k = 0.9$, sinistral shear sense) for Sanderson and Marchini model. Lineation switches instantaneously from horizontal to vertical with increasing strain. During pure shear dominated transpression ($0 < W_k \leq 0.81$), lineations are always vertical. Note that for a particular strain magnitude, lineations do not vary across the deformation zone. Predicted rock fabrics (foliation and lineation) are represented in Fig. 1. (c) Model by Robin and Cruden (1994) that includes a no-slip condition in the vertical direction as well as the horizontal direction. Lineation orientations are the same as in the Sanderson and Marchini model within the center of the deformation zone. For a particular strain magnitude, foliations and lineations vary systematically between the wall rocks and the center of the transpressed zone due to boundary effects. Fabric also varies in the vertical (X_3) direction. (d) Schematic stereonet showing lineation orientation (based on Dutton, 1997) for a wrench dominated transpression in the Robin and Cruden model at an arbitrary height (X_3 direction) within the deformation zone. Lineation orientation changes across the deformation zone and with accumulated strain. Arrows point from edge of deformation zone to center for each of the two deformation increments shown. Two strain increments are shown. Closed circles indicate lower strain increment; open squares indicate higher strain increment. (e) Triclinic deformation as described by Jones and Holdsworth (1998). Simple shear component of strain has elements of motion parallel to both X_3 and X_1. (f) Stereonet shows one example of lineation orientation with increasing strain ($\phi = 20°$, $W_k = 0.8$, sinistral shear sense) for this triclinic transpression. Note that for a particular strain magnitude, lineations do not vary across the deformation zone. Predicted rock fabrics (foliation and lineation) are represented in Fig. 9.

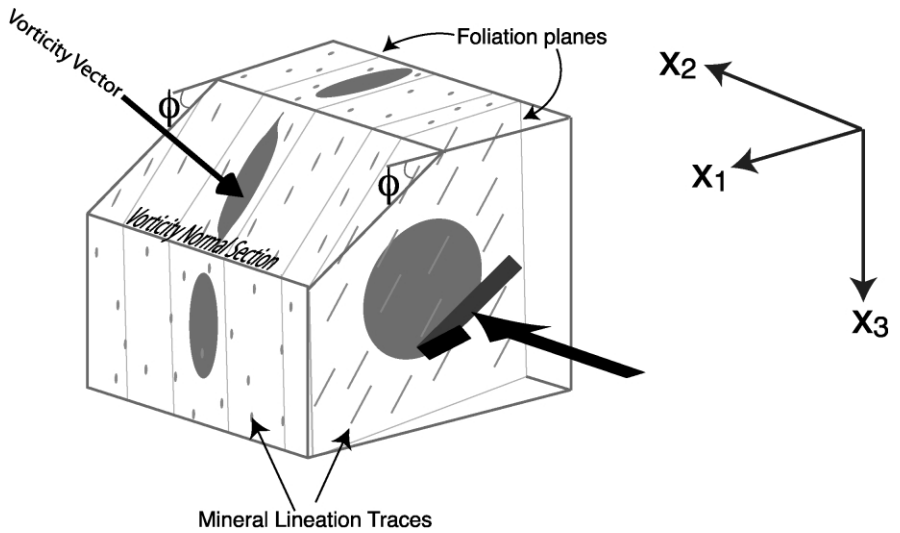

Fig. 9. Transpression strain and fabrics: triclinic model. The front (right) side of the box shown is parallel to the deformation zone boundary. ϕ = angle between the simple shear component of motion and the strike of the shear zone. The pure shear component is parallel to the X_2 direction. Ellipses represent schematic clast traces on each plane.

plunging lineation to a subvertical lineation following what approximates a small circle on a stereoplot (Fig. 10). For this reason, the deformations described by $\dot{\gamma}/\dot{\epsilon} = 2$, 4, 6, and 20 for triclinic transpression could be inferred to be strongly simple shear influenced, but not 'simple shear dominated'.

The Jones and Holdsworth/Lin et al. model could create the fabric shown in Fig. 9 with subvertical foliation and obliquely plunging lineations. It is important to consider, however, that for $\dot{\gamma}/\dot{\epsilon} \lesssim 3$, or $W_k \lesssim 0.83$, the final lineations formed are essentially subvertical *regardless of the angle* ϕ. The trend towards subvertical lineations is further enhanced with increasing strain due to the dominance of coaxial strain in generating the final fabric. As expected, in the strongly wrench-influenced transpression modeled, the lineations become increasingly more vertical with larger strains. Thus, the triclinic transpression model accounts for noticeably obliquely plunging lineations

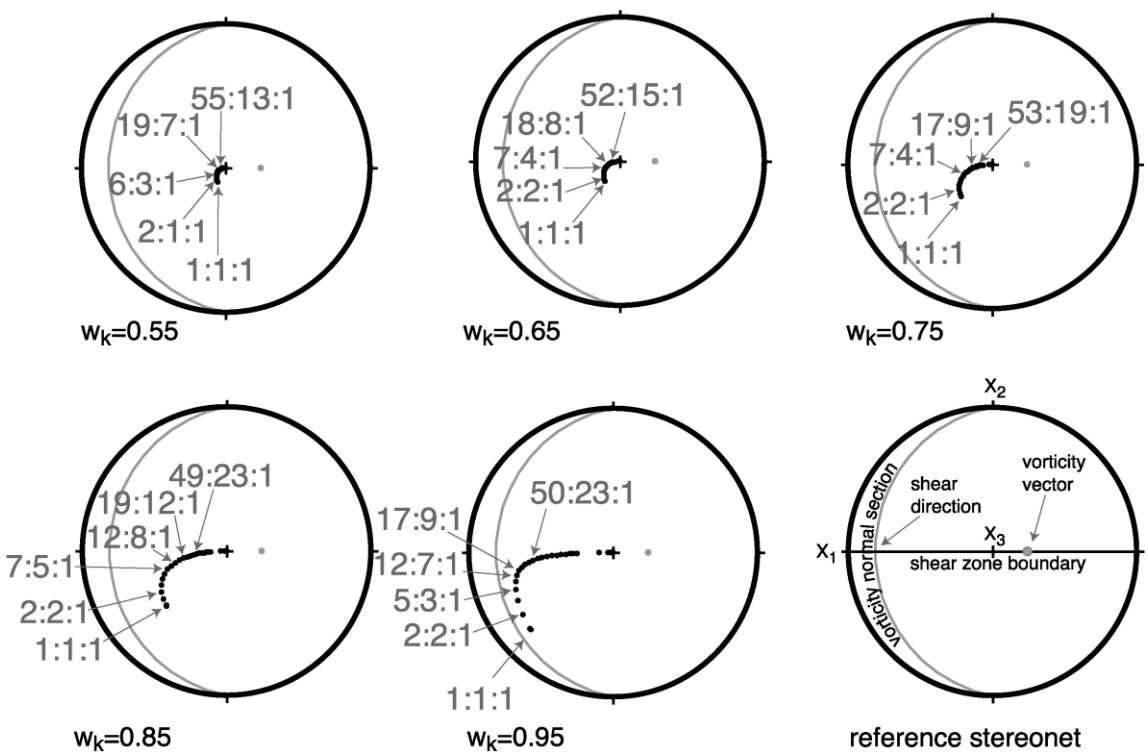

Fig. 10. Equal area stereonets indicating calculated lineation (X = long principal axis of strain ellipsoid) orientation for some representative W_k values. Selected lineations are drawn with their corresponding principal strain axes indicated. Example shown is for $\phi = 20°$ with dextral shear sense.

only during early stages of strongly wrench-influenced transpression.

Using the deformation matrix (Eq. (1)), strain orientation and magnitudes can be calculated for various values of W_k (e.g. Fig. 10 for $\phi = 20°$). While only results for $\phi = 20°$ are shown here, in all cases, as the fabric is eventually dominated by the pure shear component, lineations steepen with increasing strain.

3.2.2. Orientation of vorticity vector

The vorticity-normal section, or the plane with the highest degree of asymmetry (e.g. Robin and Cruden, 1994; Goodwin and Williams, 1996), can be estimated based on field information. This is useful for comparing field data with theoretical models. Thus, we explicitly define the orientation of the vorticity vector, the vector perpendicular to the vorticity-normal section, for the proposed triclinic model.

Using the velocity gradient tensor, **L**, we can calculate the orientation of the vorticity vector, **W**:

$$\mathbf{W} \equiv curl\mathbf{L}. \tag{3}$$

Note that this is the vorticity in an external framework. It is the vorticity in an internal framework that is important for fabric development. In the current analysis for the proposed triclinic model (not incorporating a no-slip boundary condition), these two are the same:

$$\mathbf{L} = \begin{bmatrix} \frac{\partial \nu_1}{\partial x_1} & \frac{\partial \nu_1}{\partial x_2} & \frac{\partial \nu_1}{\partial x_3} \\ \frac{\partial \nu_2}{\partial x_1} & \frac{\partial \nu_2}{\partial x_2} & \frac{\partial \nu_2}{\partial x_3} \\ \frac{\partial \nu_3}{\partial x_1} & \frac{\partial \nu_3}{\partial x_2} & \frac{\partial \nu_3}{\partial x_3} \end{bmatrix}, \tag{4}$$

and

$$\mathbf{W} = \left(\frac{\partial \nu_3}{\partial x_2} - \frac{\partial \nu_2}{\partial x_3}\right)\hat{\mathbf{x}}_1 + \left(\frac{\partial \nu_3}{\partial x_1} - \frac{\partial \nu_1}{\partial x_3}\right)\hat{\mathbf{x}}_2 + \left(\frac{\partial \nu_2}{\partial x_1} - \frac{\partial \nu_1}{\partial x_2}\right)\hat{\mathbf{x}}_3 \tag{5}$$

where $\hat{\mathbf{x}}$ are directional vectors.

The velocity gradient for the described triclinic transpression is (Lin et al., 1998, their Eq. 3):

$$\mathbf{L} = \begin{bmatrix} 0 & \dot{\gamma}\cos\phi & 0 \\ 0 & -\dot{\epsilon} & 0 \\ 0 & \dot{\gamma}\sin\phi & \dot{\epsilon} \end{bmatrix}. \tag{6}$$

Using Eqs. (4) and (5), the vorticity vector for triclinic transpression can be shown to be within the $\hat{\mathbf{x}}_1\hat{\mathbf{x}}_3$ plane, perpendicular to the plane of simple shear.

$$\mathbf{W} = (\dot{\gamma}\sin\phi)\hat{\mathbf{x}}_1 + (\dot{\gamma}\cos\phi)\hat{\mathbf{x}}_3. \tag{7}$$

Therefore, **W** is normal to the simple shear direction. The attitude of the vorticity vector and vorticity-normal section are shown in Fig. 9.

4. Application of the triclinic model to the field area

While any of the general obliquely plunging lineation models may be appropriate in different cases, it is important to be able to test the validity of the models in specific field settings, such as the Wabigoon–Quetico subprovince boundary. For reasons stated earlier, we only further consider the triclinic model (Jones and Holdsworth, 1998; Lin et al., 1998) here.

While theoretical predictions are exact, field measurements have inherent imprecision. For this reason, we consider our field observations to provide broad constraints rather than precise quantities while evaluating the model.

4.1. Range of stretching lineations

A distinguishing feature of the fabric within the Wabigoon–Quetico boundary area is the range of stretching lineations present. While the lineations plunge mostly to the east, there is a significant portion that plunge to the west. Moreover, these lineations do not appear to group into any distinctive subsets, but rather span the entire possible range of lineation orientations within the foliation plane (Fig. 4).

The triclinic model described by Lin et al. (1998) was developed with homogeneous strain. Therefore, it predicts an obliquely plunging lineation orientation that is fixed across the boundary. That is, at any instant in time with this model, there will be no variation of lineation orientation with position in the shear zone. However, if we consider this model and include deviations from homogeneous strain, the range of obliquely plunging lineations may be explained. Strain partitioning in the different forms of heterogeneities in strain orientation, magnitude, and partitioning between pure shear and simple shear across the boundary, if they exist, will create a range of obliquely plunging lineations in space as well as time.

The existence of distinct boundary segments and corresponding numerous shear directions along the transpression zone (e.g. Jones and Tanner, 1995), would result in domains of consistent obliquely plunging lineations. If indeed, boundary segments were responsible for the variation in lineation plunge obliquity along the Wabigoon–Quetico boundary, the wide range of lineation orientations along the boundary area would require that the angle ϕ had to vary significantly between segments. A large variation in ϕ seems unlikely given the relatively straight, vertical boundary; so another mechanism for producing a range of lineation plunge is required. In addition, the observation that the vorticity vector is everywhere subvertical inhibits large variability in ϕ.

If variations in strain magnitude were responsible for producing variations in lineation plunge obliquity, the zones

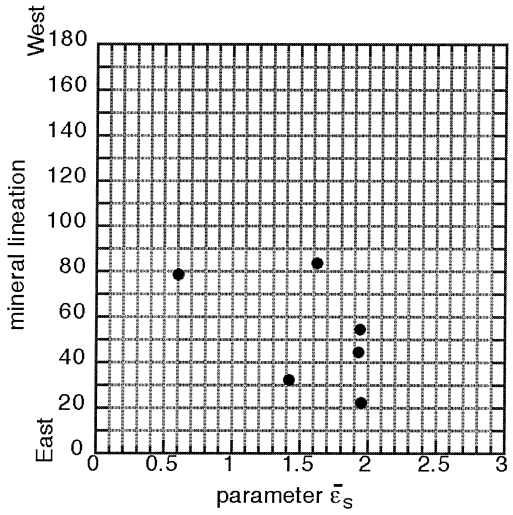

Fig. 11. Relationship between lineation plunge in degrees (0° = east, 180° = west) and deformation intensity for Seine River Conglomerates. Deformation intensity is plotted as the parameter $\bar{\varepsilon}_s$ (e.g. Hossack, 1968).

of highest strains should have the steepest lineations. Data for the Wabigoon–Quetico boundary show no such correlation between amount of strain and lineation orientation (Fig. 11), so variable strain magnitude by itself also seems an unlikely mechanism for producing a wide range of lineations.

The most likely way to achieve a range of obliquely plunging lineations along the Wabigoon–Quetico boundary within the context of the described triclinic model is through a variation in the partitioning of simple shear and pure shear throughout the zone, possibly related to the locations of the discrete shear zones. Even if this were the case, however, the Wabigoon–Quetico boundary displays both east and west plunging lineations. Without changing the sense of relative upward movement of the crustal blocks, it is difficult to generate both east and west plunging lineations by varying the angle ϕ without also changing the sense of shear. There is no field evidence to support such a change in shear sense.

In any case, if the triclinic model is appropriate for this field setting, the structural fabrics need to be consistent with the model within one outcrop. We will address this issue before we explore deviations due to strain partitioning further.

4.2. Constraining possible triclinic model deformations

For a particular location, we are able to test the triclinic model by combining multiple and independently collected pieces of fabric evidence: namely, the orientation of the vorticity-normal section, lineation plunge, and strain magnitude.

The following section gives details on a methodology to test the triclinic model in four steps. Depending on the available field information, any combination of these steps can be conducted.

4.2.1. Constraining possible triclinic model deformations: orientation of vorticity-normal section

One of the primary fabric features that can be used to constrain possible models is the orientation of the vorticity vector with respect to the shear zone boundary. In the described triclinic model, the vorticity vector is oriented perpendicular to the plane containing the simple shear vector, the vorticity-normal section. Using field evidence such as asymmetric shear sense indicators, we can approximate the vorticity-normal section by finding the plane with the maximum amount of fabric asymmetry (Goodwin and Williams, 1996). We assume that the maximum amount of fabric asymmetry is found on the vorticity-normal plane. From field observations at the Wabigoon–Quetico boundary, the asymmetric sigma and delta clasts are found most prominently on planes that are subhorizontal regardless of the lineation orientation (Fig. 5). There is no evidence, such as a metamorphic gradient across the boundary, to suggest that the whole boundary had been tilted. Because of this and in the absence of evidence for later tilting, we infer that the vorticity vector was subvertical during deformation and that the simple shear component of strain (vorticity-normal section) was restricted to a subhorizontal plane. A conservative conclusion resulting from the apparently horizontal vorticity-normal section is that the angle ϕ between the strike of the shear zone boundary and the orientation of the simple shear component was less than approximately 20° for the deformation at the Wabigoon–Quetico boundary. This limiting parameter is indicated in Step 1 of Fig. 12, which illustrates how the various lines of evidence provide constraints on the model. Because of this constraint, we will limit additional discussion to $0° < \phi < 20°$ for our application of the triclinic model to this particular field area.

4.2.2. Constraining possible triclinic model deformations: mineral lineation plunge

Our next step to constrain possible triclinic model deformations is by using the lineation plunge. In most field situations, t from Eq. (1) is unknown, but we can place some field constraints on the model based on the lineation orientation predicted for instantaneous strain and the predicted changes in orientation lineation with increasing deformation. For a given W_k and angle ϕ, we can predict the orientation of the longest axis of the strain ellipsoid (stretching lineation) for instantaneous strain (Fig. 13) using the general deformation matrix for the described triclinic transpression (Eqs. (1) and (2)) and a very small value of t. Using the same equation with increasingly larger values of t, we can predict the changing orientation of the stretching (finite) lineation. As strain accumulates, the pure shear component of strain becomes more influential and the finite lineation steepens. If such a procedure is conducted for all possible values of W_k and angle ϕ, it can be demonstrated that in each case, the instantaneous lineation plunge at the initiation of deformation is the most shallowly plunging

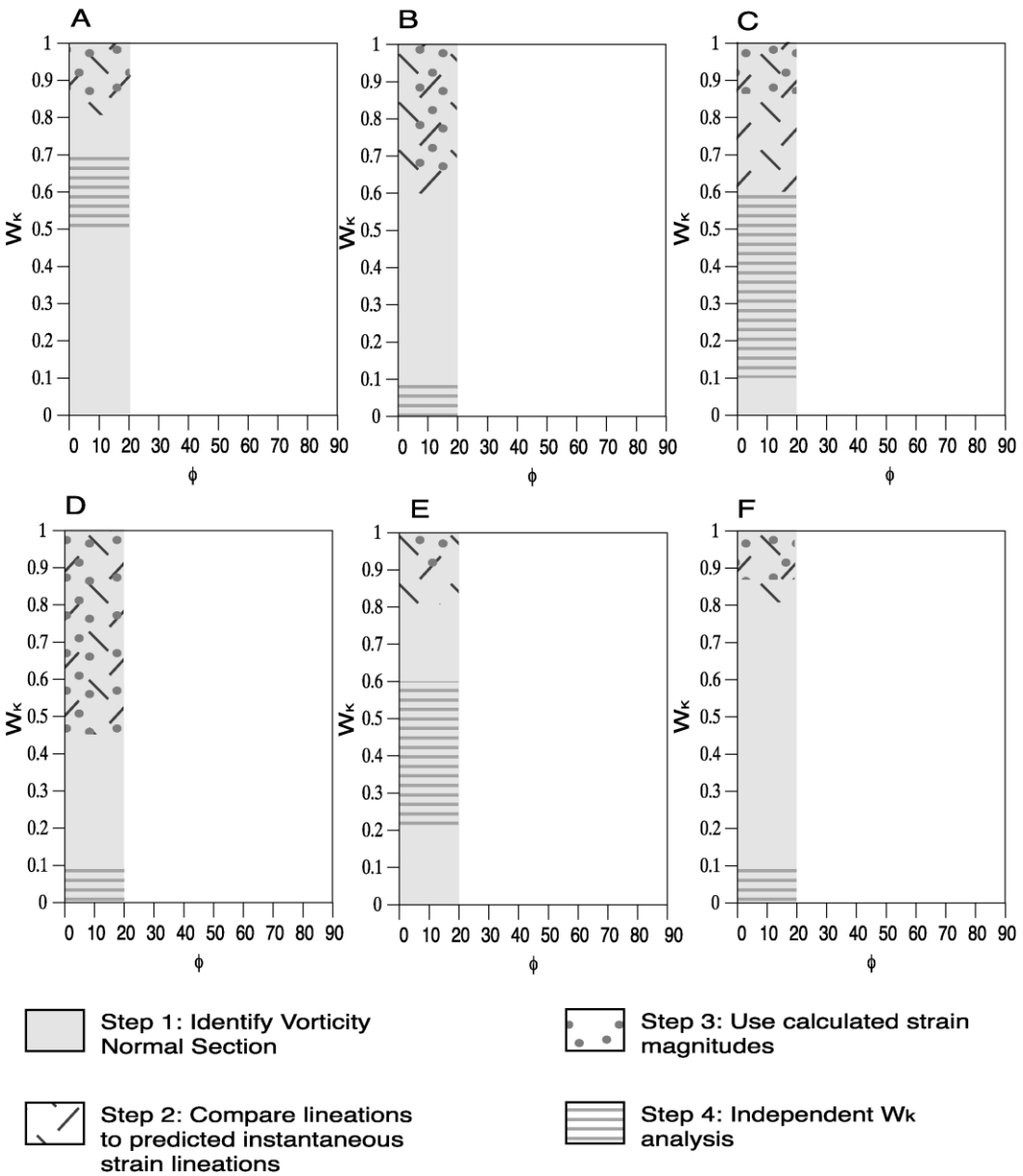

Fig. 12. All possible triclinic transpression deformations described by W_k and ϕ. Each step that was used to limit possibilities of W_k and ϕ is shown for individual outcrops. The only possible triclinic deformations (defined by W_k and ϕ) that could be responsible for the fabric at each outcrop are found by the overlap of all four steps. In the case of the six locations studied here, there is no possible overlap, thus eliminating the application of the described triclinic model to this field setting.

lineation possible for that W_k and angle ϕ. Thus, we know that the mineral lineation (which represents some accumulation of finite strain) cannot be more shallowly plunging than the instantaneous lineation in triclinic transpression. Therefore, if we know the instantaneous lineation orientation for all values of W_k and ϕ (as shown in Fig. 13), we can rule out possibilities of those triclinic transpressions that have initial instantaneous lineations that are more shallowly plunging than the measured field lineation.

For example, at outcrop C, the mineral lineation orientation is 063/54°. Throughout our field area, the attitude of the approximate vorticity-normal section in the field $\leq 20°$, so we will confine this step of our analysis to $\phi \leq 20°$ for all outcrops. Assuming a homogeneous triclinic transpression as described in Eq. (1), and using the constraint that $\phi \leq 20°$, we can infer that the rocks at this location could not have been deformed under conditions of $W_k \lesssim 0.8$ because the theoretical instantaneous lineations for all $W_k < 0.80$ plunge at greater than 54°. Thus W_k must have been greater than 0.80 at location C. This is an important conclusion because it indicates that if this transpressional model were applicable, only moderately to highly wrench-influenced transpressions could have been the cause of the fabric at location C. For other outcrops, we can similarly use the lineation orientation predicted by

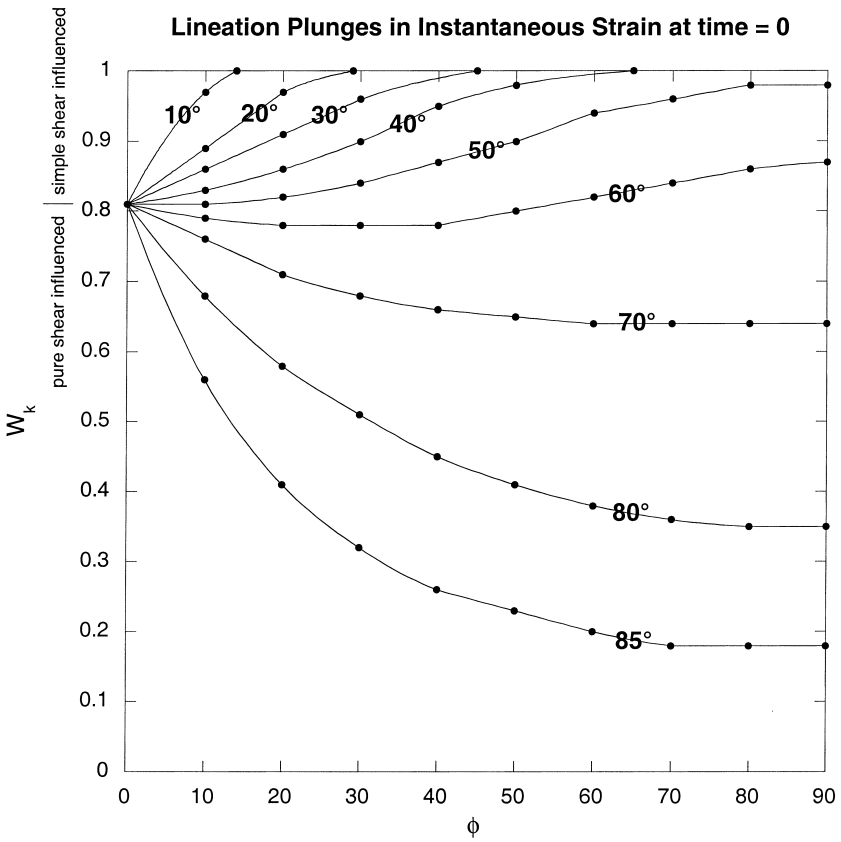

Fig. 13. Calculated values for instantaneous lineation (X) plunges for values of W_k and angle ϕ. These directions are the most shallowly plunging lineations possible for given W_k and ϕ values. As strain accumulates, lineations steepen.

instantaneous triclinic transpression with $\phi \leq 20°$ (we have already determined that $\phi \leq 20°$ for our field area). The results are shown in Step 2 of Fig. 12.

4.2.3. Constraining possible triclinic model deformations: finite strain lineation plunge

By using the conglomerates as strain recorders, we can go a step further by using the finite strain (Table 1) to find the possible t. At each outcrop, we can further limit the possible W_k and ϕ combinations by finding the best fit between the strain ellipsoid measured in the field to that predicted for each t. Using Eq. (1), we can predict the strain ellipsoid shape and orientation for each increment of triclinic transpression given an angle ϕ and values of W_k. If the strain measurements were absolutely correct, the finite strain ellipsoid would correspond to a limited set of possible W_k and ϕ for a deformed object. In this scenario, we could completely describe any triclinic transpression (W_k, ϕ) responsible for a resulting fabric, greatly limiting the possibilities. However, due to the inherent imprecision of strain analysis, we must consider the strain magnitudes listed in Table 1 to be approximate rather than definite, and we choose to limit the possible triclinic transpressions more cautiously as follows. The lineation measured in the field can be compared with the theoretical lineation based on the calculated finite strain. We choose to limit the possible triclinic transpressions (defined by W_k and ϕ) by concluding that the field-measured lineation should not be more shallowly plunging than the theoretically predicted lineation for a given finite strain magnitude.

Along the Wabigoon–Quetico boundary, we have concluded from the asymmetry of fabric elements that the angle ϕ between the shear zone boundary and the simple shear component orientation must be less than 20°. The most shallowly plunging possible lineation, therefore, will occur when ϕ is close to 0° or when $\phi = 20°$, depending on the position in W_k, ϕ space. While the following relationship is true for all increments of strain, this lineation dependence on position in W_k, ϕ space can be best illustrated during instantaneous strain (Fig. 13). Given our previous constraint that $0° \leq \phi \leq 20°$, when $W_k = 0.5$, the most shallowly plunging lineation occurs when $\phi = 20°$ for instantaneous strain (it is about 82°). Similarly, for instantaneous strain and $0° \leq \phi \leq 20°$, when $W_k = 0.9$, the most shallowly plunging lineation occurs when $\phi = 0°$ (it is horizontal).

A plot such as Fig. 13 could be drawn for further increments of strain, but is not of practical value because the 'times' such as in Eq. (1) are not apparent from rocks. However, we know that the lineations steepen with increasing strain. Therefore, a schematic plot for further strain increments would look similar to Fig. 13, except that the lines of equal lineation plunge would be shifted upwards

along the W_k axis. This means that for our field example (where we have already constrained $\phi \leq 20°$), the highest possible W_k for a given lineation plunge will either occur when ϕ is close to 0° or when $\phi = 20°$, depending on W_k. Therefore, these are the two ϕ angles we consider when analyzing possible strain paths. For each of these angles, we use Eq. (1) to predict the strain shape and orientation for each increment of triclinic transpression, given a value of W_k.

For $\phi = 20°$, the strain paths for various W_k values were calculated using Eq. (1) (Fig. 10). Using an iterative process varying 'time' and W_k, we limit the possible W_k based on a reasonable lower estimate of strain magnitude derived from our strain analysis. By only considering the $\phi = 20°$ part of the contour lines, we can limit the strain possibilities for each of the outcrops. Our results are shown in Fig. 14.

Similarly, for $\phi = 0°$, we consider the W_k number that corresponds to the instantaneous switch between horizontal and vertical lineations for a certain strain magnitude. For a very small angle ϕ at this W_k, the lineation plunge instantly changes from relatively steep to very shallow. Our results are shown in Fig. 14.

By considering the limitations for W_k imposed by both $\phi = 0°$ and $\phi = 20°$, the most conservative estimate is appropriate. For example, for location D, the estimate from $\phi = 20°$ is $W_k > 0.95$ and the estimate from $\phi = 0°$ is $W_k > 0.89$. Therefore, the overall appropriate estimate within the accepted range of ϕ is $W_k > 0.89$. Similarly, the W_k estimates for all six outcrops when considering the strain magnitudes can be found in Fig. 14, summarized in Step 3 of Fig. 12. By using this technique, we can limit the possible triclinic transpressions that might have occurred to relatively moderately to highly wrench-influenced transpressions.

4.2.4. Constraining possible triclinic model deformations: determination of vorticity number

Once the range of possible triclinic deformations is limited to a small range of W_k values, it would be useful to have an independent means to know W_k from rocks. This will allow us to further constrain the range of possible triclinic deformations. Techniques to extract W_k from deformed rocks have been summarized by Tikoff and Fossen (1995). Rocks with strain markers such as the Seine River conglomerates should be useful tools for such analysis because the strain magnitude can be calculated.

By using the horizontal component of the deformation for both monoclinic transpression ($\phi = 0°$) and triclinic transpression with $\phi = 20°$, we create plots that show the horizontal section of the strain ellipsoid, for several W_k, similar to those created by Tikoff and Fossen (1995) for other deformations (their fig. 8) (Fig. 15). The plots are constructed to show θ, the angle between the long axis of the horizontal sectional ellipse of the strain ellipsoid and the shear zone boundary, and R, the ratio between the long and short axes of the horizontal section of the strain ellipsoid.

Using our strain data (Table 1), we calculate the orientation of the horizontal section of the strain ellipsoid for each of our six representative outcrops. A sample calculation is presented in Appendix A. The shear zone boundaries for each outcrop were estimated from previous geological mapping (Wood et al., 1980a,b; Stone et al., 1997a,b) by using the geographically closest major mapped shear zone. The results for the six horizontal ellipses are plotted in Fig. 15. Values of W_k corresponding to the paired values of R and θ can be read from this plot. We assume that the error in our strain analysis measurements and shear zone boundary orientation is within 5°. Two of the measurements plot $\leq 2.5°$ below the theoretically defined curves. We assume that these measurements are essentially parallel to the shear zone boundary.

For both $\phi = 0°$ and $\phi = 20°$, the estimated vorticity numbers are similar, being slightly higher for $\phi = 20°$. The ranges of values for W_k are shown in Step 4 of Fig. 12.

From the results, it appears that the vorticity numbers, and thus the pure shear/simple shear partitioning could be very different for the six locations. There are some inherent errors in this analysis. Its accuracy depends on the accuracy of the strain measurements and the shear zone boundary orientations. Although the results of this vorticity analysis should be applied with caution, it seems unlikely that the deformation at any of these locations could have been as highly simple shear influenced as would be required by the other constraints on the described triclinic transpression model at each location (Steps 1–3 of Fig. 12). In contrast to the results from Steps 1–3, the vorticity number analysis suggests that the actual deformation was highly pure shear influenced.

4.2.5. Constraining possible triclinic model deformations: results

All possible triclinic transpression deformations (defined by W_k and ϕ) are indicated in Fig. 12. In all our steps (1–4) we have assumed a priori that the triclinic transpression model was responsible for the fabric formation in our field area. Thus, the only possible deformations, according to the described triclinic model, that could be responsible for the fabric at any one outcrop, are those corresponding to the overlap of all four steps.

Each of the four steps described in preceding sections can be used to limit the possible triclinic transpressions (defined by W_k and ϕ) that could be responsible for the deformation. Steps 1 and 2 could be done in field areas without strain markers. Step 3 requires strain markers. Step 4 requires some estimate of vorticity number, most easily accomplished with strain markers. Each of the steps has inherent error in precision, so should be used with caution. We have attempted to include reasonable error within the interpretation of each of our steps.

In the case of the six locations studied here, in not one is there an overlap of all steps. This eliminates the strict

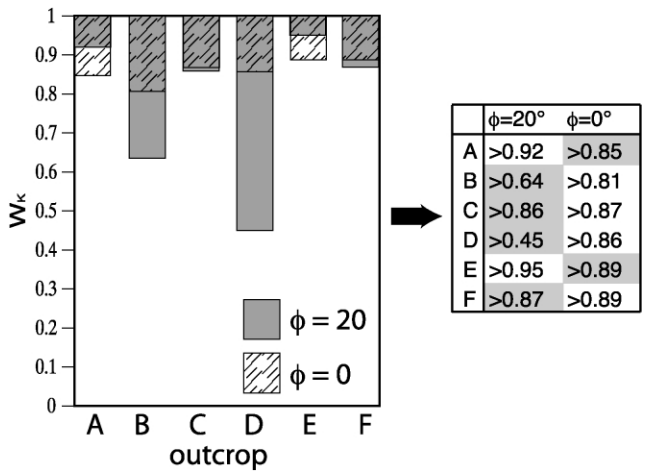

	ϕ=20°	ϕ=0°
A	>0.92	>0.85
B	>0.64	>0.81
C	>0.86	>0.87
D	>0.45	>0.86
E	>0.95	>0.89
F	>0.87	>0.89

Fig. 14. Constraining possible triclinic model deformations using finite strain lineation plunge. This table shows the results from our field area (where $\phi \leq 20°$). We choose to constrain possible triclinic models to those where the approximate stretching lineation from the calculated finite strain ellipsoid is more shallowly plunging than the stretching lineation mathematically determined by Eq. (2). In our case, the most shallowly plunging lineation for a particular W_k in the triclinic model will occur at either $\phi = 0°$ or $\phi = 20°$, so we determine the lineation plunge for each of these ϕ angles. In our case, the limiting W_k will be the one that corresponds with either $\phi = 0°$ or $\phi = 20°$, whichever is the most inclusive.

application of the described triclinic model to this field setting.

4.3. Combination model?

The Robin and Cruden/Dutton model was developed strictly for bulk monoclinic transpression, but it could be modified to account for triclinic transpression as well. Let us consider what the results would be of a theoretical model that has characteristics of both a no-slip boundary condition in the vertical direction and an inclined simple shear component. As in the monoclinic case, the center of the deformed zone (presumably the highest strain region) should be unaffected by the zones of strain and fabric transitions at the boundaries. The fabrics in the highest strained areas of the Wabigoon–Quetico boundary are not consistent with the triclinic model, so such a combination model is not an adequate explanation for the obliquely plunging lineations.

5. A new approach

The models we have examined above all produce strains and fabrics in the central part of a tectonic boundary zone that are inconsistent with key observations in the Wabigoon–Quetico boundary. These models may be appropriate for other natural examples; however, the inconsistencies with our field observations lead us to consider other ways of developing fabric, and particularly fabric variations, in a transpressional zone.

Analysis shows that, although the noncoaxial component of deformation influences strain orientation, it is the coaxial component of deformation that primarily controls the strain shape and eventually dominates its orientation (Fossen and Tikoff, 1993; Passchier, 1997; Teyssier and Tikoff, 1999). This dominance is due to the different ways in which coaxial and noncoaxial strains accumulate. In coaxial strain, the instantaneous and finite strain axes are parallel, resulting in a more efficient accumulation of strain than in noncoaxial strain, in which the instantaneous and finite strain axes are not parallel. Thus, the triclinic models described above are only effective in creating obliquely plunging lineations during the early stages of simple-shear influenced transpression. In pure-shear influenced transpression and later stages of simple-shear influenced transpression, the coaxial component of deformation dominates the finite strain. In light of this fact, a kinematic model that focuses on modifying the coaxial strain component may be more appropriate to account for obliquely plunging lineations in transpression.

The assumption in the models so far described has been that the coaxial strain component is accommodated by either vertical extrusion or horizontal extrusion parallel to the zone boundary (Fossen and Tikoff, 1993; Jones et al., 1997; Lin et al., 1998; Teyssier and Tikoff, 1999). While such extrusion seems reasonable in many situations, there is no reason that vertical extrusion should be the case, particularly at depth. The main factor that controls the direction of extrusion of ductily flowing rocks is the distribution of pressure. Perhaps in most situations, the rocks will preferentially flow upward because the pressure gradient is greatest in this direction. There are many reasons, however, that rocks at depth may not extrude in this way, especially locally. Local pressure gradients may exist due to sharp rheological contrasts. For example, flow may be diverted around a large, relatively stiff mass of rock, such as a pluton. Or there may be irregularities in the bounding shear zones that lead to local narrowing or broadening, and hence variations in pressure. Such irregularities may especially be found in rheologically diverse terranes such as the Wabigoon–Quetico boundary where there is a somewhat irregular spatial distribution of highly variable rock types from metasedimentary units to felsic to mafic metavolcanics to granitoid plutons. This variability is demonstrated on the outcrop scale very clearly by the difference in behavior of clasts of different composition in the Seine conglomerate.

Another way in which variation of strain with oblique lineations could develop, even in an originally homogeneous rock, is by strain localization into three-dimensionally anastomosing shear zones surrounding lozenges of less deformed rock (e.g. Hudleston, 1999). In such a situation, local directions of shear and of extrusion will vary and lead to non-vertical lineations. The pattern of strain and fabric produced by such a process could be very similar to that

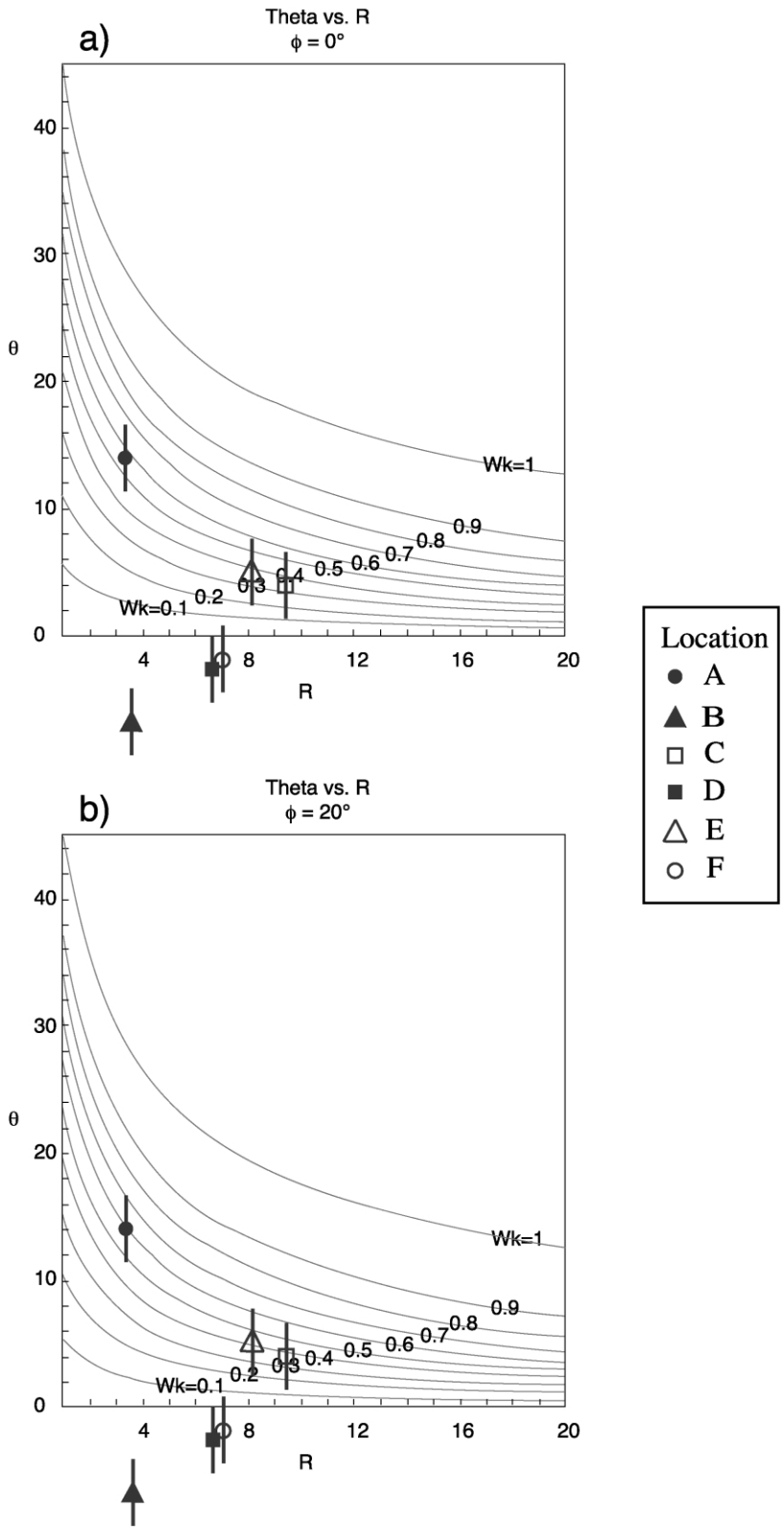

Fig. 15. Calculated ratio of horizontal strains ($R = X_h/Y_h$ where X_h and Y_h are the strain axes on the horizontal section) versus orientation of long axis (θ) of the horizontal sectional ellipse for triclinic transpression with varying W_k. (a) $\phi = 0°$. (b) $\phi = 20°$. Data from six outcrops are plotted relative to the theoretical curves. Data that lie slightly below the plot are considered to be indicative of the long axis of the strain ellipse aligned subparallel with the deformation zones.

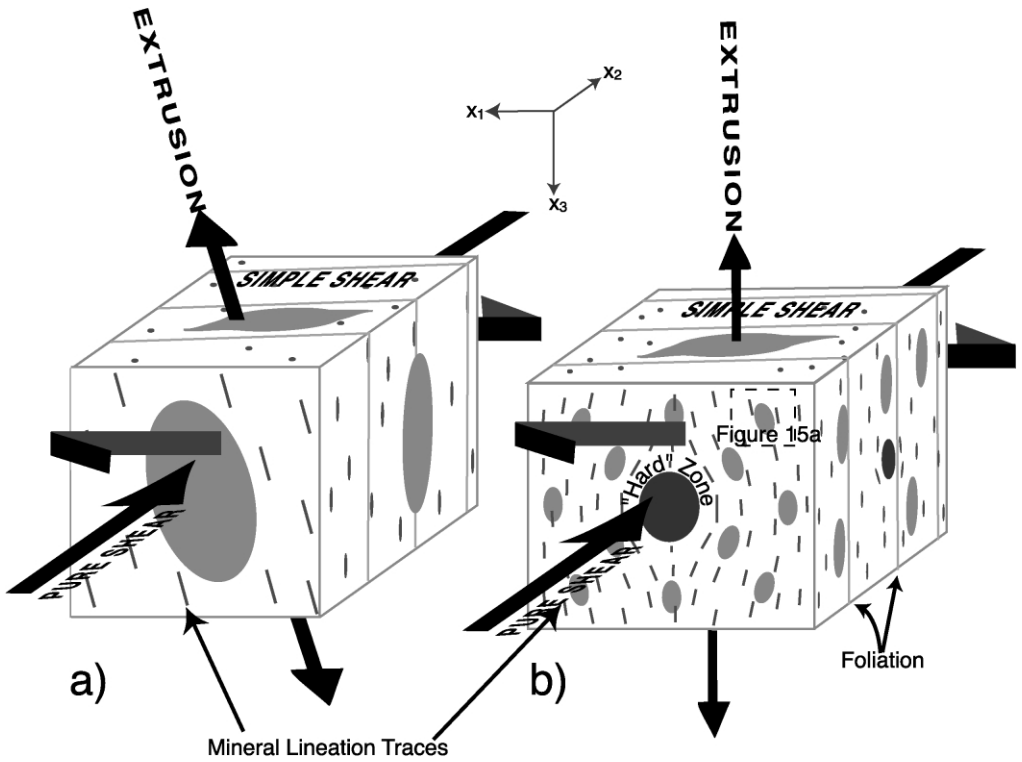

Fig. 16. Schematic view of strain and deformation fabrics for monoclinic transpression with nonvertical extrusion. Light colored ellipses represent schematic clast traces on each plane. (a) Simple view of transpression with nonvertical extrusion. (b) Schematic view of transpression with overall bulk vertical extrusion and localized zones of nonvertical extrusion. Dark colored ellipses represent schematic 'hard' zones that influence local extrusion directions. The relative location of (a) is indicated.

produced by a situation in which there are bodies of varying lithological type and thus mechanical stiffness.

In its simplest form, a model in which the direction of extrusion is non-vertical is similar to the model discussed by Jones and Holdsworth (1998) and Lin et al. (1998) in that it has triclinic symmetry, but rather than have a simple shear inclined to the horizontal, it is the pure shear component that is so inclined (oblique to X_3; Fig. 16a). However, in this basic form, as for the previously discussed triclinic and monoclinic models, only a single lineation orientation is generated for a given set of boundary conditions. That is, the strain is homogeneous. In order for the lineation orientation to vary, there must be a variation in the direction of stretch associated with the pure shear, that is the extrusion direction. This variation may be accomplished even if the overall extrusion direction remains vertical (e.g. Fig. 16b). It seems that variation in the extrusion direction about the vertical in either direction along the boundary zone is likely, and is easier to envision than a variation in the direction (inclination from horizontal) and perhaps also sense of simple shear that would be required in the Jones and Holdsworth (1998) and Lin et al. (1998) models in order to account for significant variation in the lineation plunge. Thus, in the case of the Wabigoon–Quetico boundary, non-vertical extrusion could generate both east and west plunging lineations without affecting the bulk component of simple shear, which is consistently dextral. This is illustrated in Fig. 16a, in which the extrusion direction is drawn in the X_1X_3 plane at an acute angle to the X_1 direction. A similar schematic figure could be drawn the mirror image of this one such that the extrusion direction makes an obtuse angle to the X_1 direction. These two mirror image figures represent different parts of the deforming zone in Fig. 16b. Combined, these two scenarios could generate oppositely plunging lineations without any variation in the sense of the simple shear component of deformation.

There are several reasons to suppose that deformation consistent with this form of triclinic transpression may be responsible for the fabrics developed along the Wabigoon–Quetico boundary. First, the three-dimensional anastomosing nature of the shear zones and the wide range of lithologies and resultant rheological contrasts along the boundary provide physical conditions necessary and sufficient for changing the extrusion direction. Second, the presence of both east and west plunging lineations is most readily explainable by developing zones of variable and local non-vertical extrusion. On average, the net extrusion direction is likely to be vertical, or nearly so. Lastly, the variations in the amount of strain are inherent to this localized non-vertical extrusion model.

6. Summary and conclusions

We have presented a step-by-step approach for testing the

ability of published triclinic transpression models to account for obliquely plunging lineations. Each step independently constrains the possible values of kinematic vorticity, W_k, or angle of inclination of simple shear to the horizontal (ϕ) that could have been responsible for a subset of the observed structural and fabric characteristics in a zone of suspected quasi transpressional deformation. Depending on the nature and amount of field evidence available, different combinations of these steps may be used, and the more steps that are used, the greater the confidence in the results. The results in each case are in the form of permissible ranges in the values of W_k and ϕ. In order to accept triclinic transpression as a possible kinematic framework for interpreting the structures and fabric, the ranges in values of W_k and ϕ must show mutual consistency. If there is significant inconsistency, the triclinic model is ruled out.

Existing models, such as those that modify frictional boundary conditions (Robin and Cruden, 1994; Dutton, 1997) or those of bulk triclinic symmetry (Jiang and Williams, 1998; Jones and Holdsworth, 1998; Lin et al., 1998), cannot explain the obliquely plunging lineations within the Wabigoon–Quetico boundary zone because they are not consistent with all of the field observations. The obliquely plunging lineations cannot be explained by these models because: (1) they occur throughout the deformation zone, rather than just at the edges; (2) the lineations vary from their predicted values in many places where the foliations do not; (3) the apparent orientation of the vorticity vector is subvertical, which effectively limits possibilities for inclined simple shear; (4) lineations vary seemingly irregularly along the boundary and with finite strain suggesting that the obliquity is not consistent within a series of boundary segments or panels with fixed values of W_k and ϕ, with or without variation in finite strain magnitude; (5) when the measured strain magnitude is compared with the strain predicted for triclinic transpression, the observed lineation orientation is inconsistent with the lineation orientation predicted by the model for this strain, unless W_k is high; (6) the estimates of W_k from strain calculations at all the locations studied are lower than those required by the triclinic model; and (7) the range of lineation plunge (both east and west) is unlikely to occur in the described triclinic model.

From the observations on strain and fabric and their mutual incompatibility with the triclinic models, it is clear that another approach is needed to account for obliquely plunging lineations in transpression. The most promising approach may be one in which the direction of extrusion is non-vertical and variable, while the direction and sense of simple shear is constant and sub-horizontal. The physical conditions that might lead to such behavior include variation in lithology and thus rock stiffness in the boundary zone, variation in the orientation of bounding shear zones, and strain localization. It seems in particular that variation in the extrusion direction may account most readily for the presence of both east and west plunging lineations in the Wabigoon–Quetico boundary zone.

Acknowledgments

A. Yonkee graciously provided the three-dimensional strain program. DMC received student research grants from Sigma Xi, the University of Minnesota Department of Geology and Geophysics, the Geological Society of America, and the University of Minnesota Doctoral Dissertation Special Grants program that were used to conduct the field work for our study. Sandy Cruden and Sue Treagus provided very thoughtful and helpful reviews that greatly improved the manuscript.

Appendix A

Appendix

The following is a sample calculation for outcrop C (moderate strain).

Change ellipsoid from ellipsoidal coordinates x, y, z into geographic coordinates, $\hat{x}, \hat{y}, \hat{z}$ (east, north, down):

$$\left\{\begin{array}{l} 6.75x = 3.76\hat{x} + 1.76\hat{y} + 5.32\hat{z} \\ 4y = -3.12\hat{x} - 0.44\hat{y} + 2.46\hat{z} \\ 0.5z = 0.12\hat{x} - 0.48\hat{y} + 0.07\hat{z} \end{array}\right\}. \quad \text{(A1)}$$

Equation for ellipsoid in its own reference frame:

$$\frac{x^2}{45.56} + \frac{y^2}{16.00} + \frac{z^2}{0.25} = 1. \quad \text{(A2)}$$

Solve for x, y, z in terms of $\hat{x}, \hat{y}, \hat{z}$.

$$\frac{(3.76\hat{x} + 1.76\hat{y} + 5.32\hat{z})^2}{(6.75)^2(45.56)} + \frac{(-3.12\hat{x} - 0.44\hat{y} + 2.46\hat{z})^2}{(4)^2(16.00)} + \frac{(0.12\hat{x} - 0.48\hat{y} + 0.07\hat{z})^2}{(0.5)^2(0.25)} = 1. \quad \text{(A3)}$$

Horizontal section where $z = 0$; simplify:

$$\frac{(3.76\hat{x} + 1.76\hat{y})^2}{2075.94} + \frac{(-3.12\hat{x} - 0.44\hat{y})^2}{256.00} + \frac{(0.12\hat{x} - 0.48\hat{y})^2}{0.06} = 1. \quad \text{(A4)}$$

$$\frac{(3.76\hat{x} + 1.76\hat{y})^2 + 8.11(-3.12\hat{x} - 0.44\hat{y})^2 + 34599(0.12\hat{x} - 0.48\hat{y})^2}{2075.94} = 1. \quad \text{(A5)}$$

$$591.3\hat{x}^2 - 2(1975.14)\hat{x}\hat{y} + 7976.28\hat{y}^2 - 2075.94 = 0. \quad \text{(A6)}$$

In matrix form:

$$x'Ax - 2075.94 = 0. \qquad A = \begin{bmatrix} 591.30 & -1975.14 \\ -1975.14 & 7976.28 \end{bmatrix}. \quad \text{(A7)}$$

Solving for the square roots of eigenvalues of A results in the axes lengths of the horizontal section ellipse: (92.04, 9.81) or (9.38, 1) The eigenvectors give the orientations of those horizontal axes: directions 76° and 166°.

References

Bauer, R.L., 1985. Correlation of early recumbent and younger upright folding across the boundary between an Archean gneiss belt and greenstone terrane, northeastern Minnesota. Geology 13, 657–660.

Bilby, B.A., Kolbuszewski, M.L., 1977. The finite deformation of an inhomogeneity in two-dimensional slow viscous incompressible flow. Proceedings of the Royal Society of London 355, 335–353.

Bilby, B.A., Eshelby, J.D., Kundu, A.K., 1975. The changes in shape of a viscous ellipsoidal region embedded in a slowly deforming matrix having a different viscosity. Tectonophysics 28, 265–274.

Borradaile, G.J., Dehls, J.F., 1993. Regional kinematics inferred from magnetic subfabrics in Archean rocks of northern Ontario, Canada. Journal of Structural Geology 15, 887–894.

Borradaile, G.J., Werner, T., Dehls, J.F., Spark, R.N., 1993. Archean regional transpression and paleomagnetism in northwestern Ontario, Canada. Tectonophysics 220, 117–125.

Burke, K., Dewey, J.F., Kidd, W.S.F., 1976. Dominance of horizontal movements, arc and microcontinental collisions during the later permobile regime. In: Windley, B.F., (Ed.), The Early History of the Earth, pp. 113–129.

Card, K.D., 1990. A review of the Superior Province of the Canadian Shield, a product of Archean accretion. Precambrian Research 48, 99–156.

Card, K.D., Ciesielski, A., 1986. DNAG Subdivisions of the Superior Province of the Canadian Shield. Geoscience Canada 13, 5–13.

Czeck, D.M., 2001. Strain Analysis, Rheological Constraints, and Tectonic Model for an Archean Polymictic Conglomerate: Superior Province, Ontario, Canada. Ph.D. thesis, University of Minnesota.

Davis, D.W., Poulsen, K.H., Kamo, S.L., 1989. New insights into Archean crustal development from geochronology in the Rainy Lake area, Superior Province, Canada. Journal of Geology 97, 379–398.

Dutton, B.J., 1997. Finite strains in transpression zones with no boundary slip. Journal of Structural Geology 19, 1189–1200.

Eshelby, J.D., 1957. The determination of the elastic field of an ellipsoidal inclusion, and related problems. Proceedings of the Royal Society of London A241, 376–396.

Etheridge, M.A., Vernon, R.H., 1981. A deformed polymictic conglomerate; the influence of grain size and composition on the mechanism and rate of deformation. Tectonophysics 79, 237–254.

Flinn, D., 1965. On the symmetry principle and the deformation ellipsoid. Geological Magazine 102, 36–45.

Fossen, H., Tikoff, B., 1993. The deformation matrix for simultaneous simple shearing, pure shearing and volume change, and its application to transpression–transtension tectonics. Journal of Structural Geology 15, 413–422.

Fralick, P., Davis, D., 1999. The Seine–Coutchiching problem revisited: sedimentology, geochronology and geochemistry of sedimentary units in the Rainy Lake and Sioux Lookout Areas. In: Harrap, R.M., Helmstaedt, H. (Eds.), 1999 Western Superior Transect Fifth Annual Workshop 70, pp. 66–75.

Frantes, J.R., 1987. Petrology and sedimentation of the Archean Seine Group conglomerate and sandstone, Western Wabigoon Belt, Northern Minnesota and Western Ontario. M.S. thesis, University of Minnesota.

Freeman, B., 1987. The behaviour of deformable ellipsoidal particles in three-dimensional slow flows: implications for geological strain analysis. Tectonophysics 132, 297–309.

Freeman, B., Lisle, R.J., 1987. The relationship between tectonic strain and the three-dimensional shape fabrics of pebbles in deformed conglomerates. Journal of the Geological Society of London 144, 635–639.

Gay, N.C., 1968a. Pure shear and simple shear deformation of inhomogeneous viscous fluids. 1. Theory. Tectonophysics 5, 211–234.

Gay, N.C., 1968b. Pure shear and simple shear deformation of inhomogeneous viscous fluids. 2. The determination of the total finite strain in a rock from objects such as deformed pebbles. Tectonophysics 5, 295–302.

Gay, N.C., 1969. The analysis of strain in the Barberton Mountain Land, Eastern Transvaal, using deformed pebbles. Journal of Geology 77, 377–396.

Goodwin, L.B., Williams, P.F., 1996. Deformation path partitioning within a transpressive shear zone, Marble Cove, Newfoundland. Journal of Structural Geology 18, 975–990.

Harland, W.B., 1971. Tectonic transpression in Caledonian Spitsbergen. Geological Magazine 108, 27–42.

Hoffman, P.F., 1989. Precambrian geology and tectonic history of North America. In: Bally, A.W., Palmer, A.R. (Eds.), The Geology of North America; an Overview. The Geology of North America A, pp. 447–512.

Hoffman, P.F., 1990. On accretion of granite–greenstone terrane. In: Robert, F., Sheahan, P.A., Green, S.B. (Eds.), Greenstone Gold and Crustal Evolution; NUNA Conference Volume, pp. 32–45.

Holst, T.B., 1982. The role of initial fabric on strain determination from deformed ellipsoidal objects. Tectonophysics 82, 329–350.

Hooper, P.R., Ojakangas, R.W., 1971. Multiple deformation in Archean rocks of the Vermilion District, northeastern Minnesota. Canadian Journal of Earth Sciences 8, 423–434.

Hossack, J.R., 1968. Pebble deformation and thrusting in the Bygdin area (S. Norway). Tectonophysics 5, 315–339.

Huber-Aleffi, A., 1982. Strain determinations in the conglomeratic gneiss of the Lebendun Nappe, Ticino, Switzerland. Geologica Romana 21, 235–277.

Hudleston, P.J., 1999. Strain compatibility and shear zones: is there a problem? Journal of Structural Geology 21, 923–932.

Hudleston, P.J., Schultz-Ela, D.D., Southwick, D.L., 1988. Transpression in an Archean greenstone belt, northern Minnesota. Canadian Journal of Earth Sciences 25, 1060–1068.

Jiang, D., Williams, P.F., 1998. High-strain zones: a unified model. Journal of Structural Geology 20, 1105–1120.

Jones, R.R., Tanner, P.W.G., 1995. Strain partitioning in transpression zones. Journal of Structural Geology 17, 793–802.

Jones, R.R., Holdsworth, R.E., 1998. Oblique simple shear in transpression zones. In: Holdsworth, R.E., Strachran, R.A., Dewey, J.F. (Eds.), Continental Transpressional and Transtensional Tectonics. Geological Society of London, Special Publications 135, pp. 35–40.

Jones, R.R., Holdsworth, R.E., Bailey, W., 1997. Lateral extrusion in transpression zones; the importance of boundary conditions. Journal of Structural Geology 19, 1201–1217.

Langford, F.F., Morin, J.A., 1976. The development of the Superior Province of northwestern Ontario by merging island arcs. American Journal of Science 276, 1023–1034.

Lin, S., Jiang, D., Williams, P.F., 1998. Transpression (or transtension) zones of triclinic symmetry: natural example and theoretical modeling. In: Holdsworth, R.E., Strachran, R.A., Dewey, J.F. (Eds.), Continental Transpressional and Transtensional Tectonics. Geological Society of London, Special Publications 135, pp. 41–57.

Lisle, R.J., 1979. Strain analysis using deformed pebbles; the influence of initial pebble shape. Tectonophysics 60, 263–277.

Lisle, R.J., 1985. Geological Strain Analysis: A Manual for the Rf/ϕ Method, Pergamon Press, Oxford.

Lisle, R.J., Rondeel, H.E., Doorn, D., Brugge, J., Van de Gaag, P., 1983. Estimation of viscosity contrast and finite strain from deformed elliptical inclusions. Journal of Structural Geology 5, 603–610.

Merle, O., Gapais, D., 1997. Strains within thrust–wrench zones. Journal of Structural Geology 19, 1011–1014.

Owens, W.H., 1984. The calculation of a best-fit ellipsoid from elliptical sections on arbitrarily orientated planes. Journal of Structural Geology 6, 571–578.

Passchier, C.W., 1997. The fabric attractor. Journal of Structural Geology 19, 113–127.

Poulsen, K.H., 1986. Rainy Lake Wrench Zone: an example of an Archean Subprovince boundary in Northwestern Ontario. In: de Wit, M.J., Ashwal, L.D. (Eds.), Tectonic Evolution of Greenstone Belts Technical Report 86-10, pp. 177–179.

Poulsen, K.H., Borradaile, G.J., Kehlenbeck, M.M., 1980. An inverted Archean succession at Rainy Lake, Ontario. Canadian Journal of Earth Sciences 17, 1358–1369.

Ramsay, J.G., 1967. Folding and Fracturing of Rocks, McGraw-Hill, New York.

Ramsay, J.G., Huber, M.I., 1983. The Techniques of Modern Structural Geology, Academic Press, London.

Robin, P.-Y., Cruden, A.R., 1994. Strain and vorticity patterns in ideally ductile transpression zones. Journal of Structural Geology 16, 447–466.

Sanderson, D.J., Marchini, W.R.D., 1984. Transpression. Journal of Structural Geology 6, 449–458.

Schultz-Ela, D.D., Hudleston, P.J., 1991. Strain in an Archean greenstone belt of Minnesota. Tectonophysics 190, 233–268.

Shimamoto, T., Ikeda, Y., 1976. A simple algebraic method for strain estimation from deformed ellipsoidal objects; 1. Basic theory. Tectonophysics 36, 315–337.

Stone, D., Hallé, J., Murphy, R., 1997. Precambrian geology, Mine Centre area. Ontario Geological Survey Preliminary Map P. 3372, scale 1:50,000.

Stone, D., Hallé, J., Murphy, R., 1997. Precambrian geology, Mine Centre area. Ontario Geological Survey Preliminary Map P. 3373, scale 1:50,000.

Tabor, J.R., Hudleston, P.J., 1991. Deformation at an Archean subprovince boundary, northern Minnesota. Canadian Journal of Earth Sciences 28, 292–307.

Teyssier, C., Tikoff, B., 1999. Fabric stability in oblique convergence and divergence. Journal of Structural Geology 21, 969–974.

Tikoff, B., Fossen, H., 1995. The limitations of three-dimensional kinematic vorticity analysis. Journal of Structural Geology 17, 1771–1784.

Tikoff, B., Greene, D., 1997. Stretching lineations in transpressional shear zones: an example from the Sierra Nevada Batholith, California. Journal of Structural Geology 19, 29–39.

Treagus, S.H., Lan, L., 2000. Pure shear deformation of square objects, and applications to geological strain analysis. Journal of Structural Geology 22, 105–122.

Treagus, S.H., Hudleston, P.J., Lan, L., 1996. Non-ellipsoidal inclusions as geological strain markers and competence indicators. Journal of Structural Geology 18, 1167–1172.

Truesdell, C., 1954. The Kinematics of Vorticity, Indiana University Press, Bloomington.

White, J.C., 1982. Quartz deformation and the recognition of recrystallization regimes in the Flinton Group conglomerates, Ontario. Canadian Journal of Earth Sciences 19, 81–93.

Wood, J., 1980. Epiclastic sedimentation and stratigraphy in the North Spirit Lake and Rainy Lake areas; a comparison. Precambrian Research 12, 227–255.

Wood, J., Dekker, J., Jansen, J.G., Keay, J.P., Panagapko, D., 1980. Mine Centre Area (Eastern Half), District of Rainy River. Ontario Geological Survey Preliminary Map P. 2202, scale 1:15840.

Wood, J., Dekker, J., Jansen, J.G., Keay, J.P., Panagapko, D., 1980. Mine Centre Area (Western Half), District of Rainy River. Ontario Geological Survey Preliminary Map P. 2201, scale 1:15840.